



# Integrated mathematical modeling of cross-scale dynamics and equity constraints in water–energy–food systems

Mohammad Fazle Rabbi<sup>1</sup>

Received: 17 May 2025 / Accepted: 9 February 2026  
© The Author(s) 2026

## Abstract

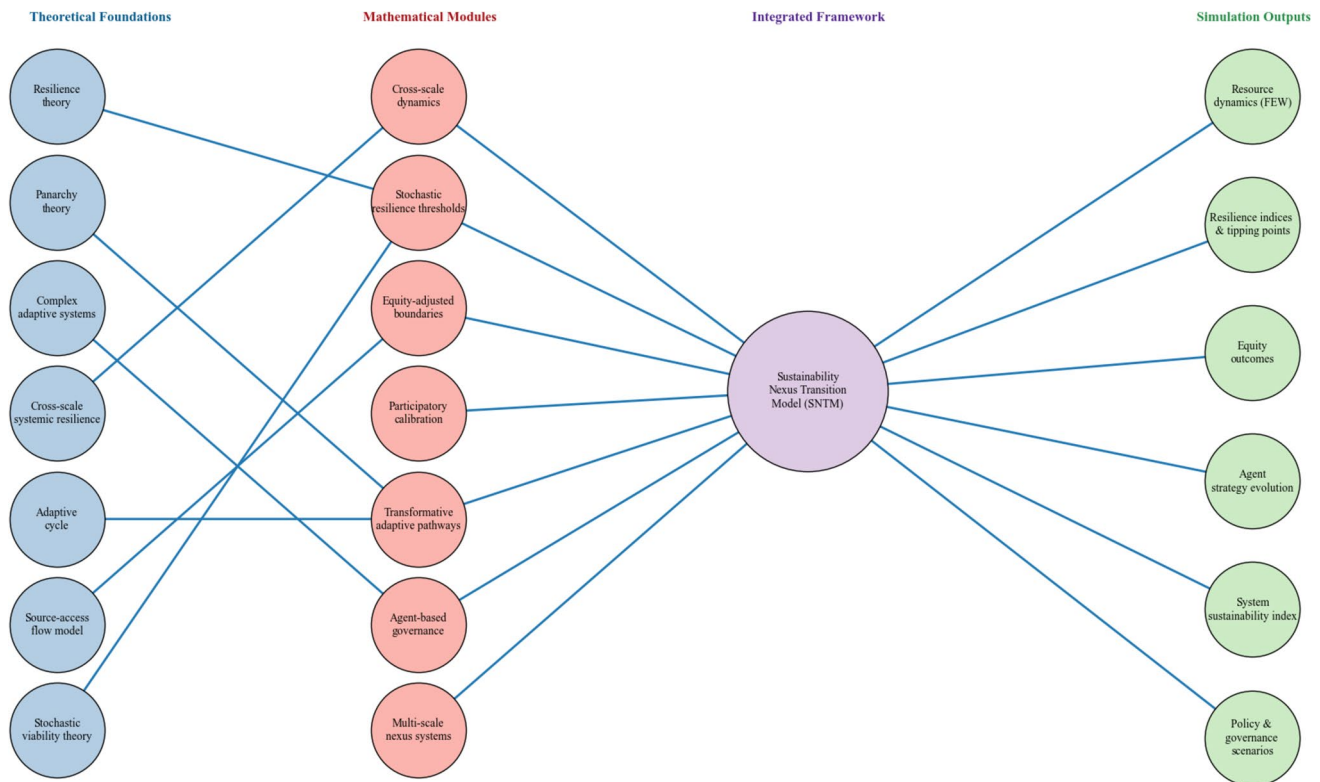
Global sustainability challenges manifest as complex system dynamics operating across multiple scales, where water, energy, and food systems interact through amplified stochastic shocks and equity constraints. Prevailing methodologies overlook cross-scale feedbacks, represent resilience as fixed, and neglect random disturbances and equity concerns, restricting their capacity to guide adaptive and just sustainability pathways. This study addresses the existing gap by introducing the Sustainability Nexus Transition Model (SNTM). As a unified mathematical framework, the SNTM synthesizes seven theoretical traditions including resilience theory, panarchy, complex adaptive systems, cross-scale systemic resilience, adaptive cycles, source-access-flow models, and stochastic viability theory, transforming these theories into a single operational system. The methodology integrates hybrid differential equations, stochastic processes, equity-constrained optimization, participatory calibration, agent-based governance, and transformative adaptive pathways to capture nonlinear dynamics, feedback amplification, and multi-actor adaptation across water–energy–food sectors. Simulation experiments across 50 independent runs reveal that local water shocks below 40% of carrying capacity trigger cascading failures, with energy flux amplifying over 170% within 20 time steps. Incorporating equity weights above 0.7 sustains system stability 89% longer than equity-agnostic models, while decentralized agent-based governance decreases recovery time by 52% compared to centralized approaches. Adaptive pathway switching lowers maladaptation risk by 58%. Sensitivity analysis confirms robustness under  $\pm 30\%$  parameter variations, and empirical validation against Murray–Darling Basin sectoral fluxes (2000–2020) demonstrates real-world applicability. The SNTM provides a platform for scenario analysis, early warning detection, and participatory policy design under deep uncertainty, contributing to sustainability science applied to water–energy–food systems by translating multi-actor processes into formal models that support equitable adaptive governance.

---

✉ Mohammad Fazle Rabbi  
drrabbikhan@gmail.com; rabbi.mohammad@econ.unideb.hu

<sup>1</sup> Coordination and Research Centre for Social Sciences,  
Faculty of Economics and Business, University of Debrecen,  
Böszörményi Út 138, Debrecen 4032, Hungary

## Graphical abstract



**Keywords** Sustainability Nexus Transition Model (SNTM) · Cross-scale dynamics · Stochastic resilience · Equity-weighted resource allocation · Adaptive governance · Water–energy–food nexus

### Abbreviations

CAS	Complex adaptive systems
CSRC-ABAL	Cross-scale resilience coupled agent-based adaptive learning
SAF	Source-access-flow (model)
SDG	Sustainable development goal
SEM	Social equity matrix
SNTM	Sustainability Nexus Transition Model
TAP	Transformative adaptive pathways
UNDP	United Nations Development Programme
UNDRR	United Nations Office for Disaster Risk Reduction
WEF	Water–energy–food (nexus)

### Introduction

Meeting the demands of sustainability in a rapidly changing world requires innovative analytical paradigms capable of addressing the complexity, dynamism, and uncertainty inherent in socio-ecological systems (Glendell et al. 2025). The growing complexity of global sustainability problems

compels the development of analytical frameworks that move beyond established disciplinary boundaries and methodological limitations (Gomes et al. 2024). These issues are not independent but rather originate from deeply interwoven processes that operate across a multitude of scales, domains, and dimensions. As interconnected crises such as intensifying climate change, accelerating biodiversity loss, resource scarcity, and deepening socio-economic inequities unfold simultaneously, they interact in nonlinear ways, amplifying systemic vulnerabilities and feedback loops (Lawrence et al. 2024; Gomes et al. 2024). Consequently, the analytical demands posed by these complex issues create significant hurdles, revealing a fundamental inadequacy in traditional disciplinary frameworks and methodological toolsets to provide comprehensive understanding or effective solutions. These legacy approaches, often rooted in reductionist paradigms, struggle to capture the dynamic interplay between system components, the cascading effects of perturbations, or the adaptive capacities of systems under stress (Quadrat-Ullah 2025; Apata 2025). While recent advances in environmental science, complex systems physics, and industrial ecology have expanded sustainability analysis (Pandey

et al. 2025; Li et al. 2025; Fu et al. 2025), and integrated approaches to water–energy–food (WEF) nexus systems have gained prominence (Vinca et al. 2021; Pukšec and Duić 2022; Saed et al. 2024; Vahabzadeh et al. 2025), the inherent nonlinearities, emergent properties, and cross-scale interactions within socio-ecological systems continue to challenge integrated modeling frameworks that must simultaneously address multiple scales, sectors, and stochastic disturbances. Many conventional approaches, particularly in economic and policy modeling, still prioritize linear relationships, assume equilibrium, or examine sectors in isolation while treating equity as exogenous to biophysical dynamics, limiting their capacity to capture system-wide dynamics and distributional justice concerns. Considering the inherent complexities, uncertainties, and dynamic nature of contemporary challenges, it becomes imperative to advance integrative, adaptive, and transdisciplinary frameworks. Such approaches are essential not only for illuminating intricate interdependencies but also for generating implementable strategies to effectively address and operate within an increasingly unpredictable future.

Sustainability science is increasingly moving toward the understanding that the converging crises observed today are not isolated events (Scarano et al. 2024). Instead, they are conceptualized as tangible outcomes of more fundamental, systemic interactions operating within the complex architecture of socio-ecological systems. These dynamics are governed by complex feedback loops, nonlinear threshold effects, and interdependencies that cut across sectors and scales. For instance, the water–energy–food nexus reveals how resource constraints in one sector can cascade through interconnected systems, leading to amplification effects that conventional single-sector models cannot capture (Rabbi and Amin 2024). Moreover, the unequal distribution of environmental risks and resources underscores the inextricable links between ecological stressors and socio-economic disparities (Rabbi 2024). The disproportionate burden of pollution, climate impacts, and resource scarcity borne by marginalized populations reveals the inherently coupled nature of biophysical and social dimensions (Kallis et al. 2025; Chakraborty et al. 2025). This complexity is often marginalized or overlooked by models that are completely technical or ecologically deterministic. Therefore, responding effectively to these dynamics necessitates more than incremental adjustments to existing methodologies; it demands the construction of fully integrated, cross-disciplinary frameworks that can capture the relational, adaptive, and multi-dimensional character of sustainability transitions. Such frameworks must be capable of illuminating not only systemic risks but also the pathways toward resilience, equity, and transformation.

While sustainability science has advanced considerably, a fundamental modeling gap still impedes progress: the lack of an integrated mathematical framework that can

simultaneously address the dynamic, multi-scale, stochastic, and socially embedded nature of sustainability challenges. This gap manifests not merely as a collection of separate methodological limitations, but as a systemic inability to capture the holistic character of sustainability transitions. Analyzing this gap through the perspective of seven core theoretical traditions such as resilience theory (Holling 1973; Walker et al. 2004), panarchy theory (Gunderson and Holling 2002), complex adaptive systems (Holland 1992; Gell-Mann 1994; Berkes et al. 2001), cross-scale systemic resilience (Walker et al. 2004; Folke et al. 2016; Williams et al. 2021), adaptive cycle (Holling 1986; Biggs et al. 2012), source-access-flow models (Dabelko 2005; Le Billon 2001; Ribot and Peluso 2003), and stochastic viability theory (De Lara and Doyen 2008; Aubin 2009; Barbrook-Johnson and Penn 2021) uncovers five critical dimensions that current approaches have yet to reconcile within a unified framework.

First, the prevalent use of deterministic equations in current sustainability models inadequately captures the inherent stochasticity and deep uncertainty of socio-ecological systems. By assuming predictable, noise-free dynamics, these models fundamentally mischaracterize systems where random fluctuations can initiate regime shifts, particularly when systems are close to critical thresholds. Second, conventional models typically treat social equity considerations as exogenous to biophysical dynamics rather than as intrinsic system parameters. This artificial separation between planetary boundaries and distributive justice concerns not only leads to ethically problematic frameworks but also results in analytically incomplete models that overlook crucial feedback loops between resource allocation and system stability.

Third, most approaches assume fixed governance structures instead of modeling adaptive, multi-level institutional responses that evolve in response to changing conditions. This static depiction of governance overlooks the dynamic interplay between formal institutions, informal norms, and emergent collective behaviors crucial to real-world sustainability governance. Fourth, sectoral models (water, energy, food) remain largely isolated, unable to capture cross-sectoral cascade effects that propagate across domains through complex coupling mechanisms (FAO 2014). As a result, these models cannot represent the transmission of stresses from one sector to another, potentially initiating system-wide instabilities through unforeseen pathways.

Fifth, traditional frameworks rely on static threshold concepts rather than dynamic, context-dependent resilience boundaries that fluctuate based on system history, governance arrangements, and cross-scale feedbacks. This oversimplification produces brittle resilience assessments that fail to account for the adaptive capacity of socio-ecological systems under varying conditions. Collectively, these limitations reveal not just technical modeling challenges but fundamental conceptual barriers to understanding sustainability

as an emergent property of complex, adaptive socio-ecological systems.

Recent empirical advances have provided critical data on cross-scale heterogeneity in water–energy–food nexus systems (Li et al. 2025) spatial heterogeneity in urban land systems (Fu et al. 2025), climate–land–energy–water nexus models across multiple scales (Vinca et al. 2021), water–energy–food nexus interactions (Saed et al. 2024; Vahabzadeh et al. 2025), and infrastructure equity dynamics (Pandey et al. 2025). However, as Schlüter et al. (2023) note, sustainability scientists rarely combine modeling with empirical approaches. This framework addresses this gap by incorporating these empirical insights into its mathematical structure and validating outputs against Murray–Darling Basin observational data (2000–2020).

Each of these five limitations such as deterministic assumptions, equity blindness, static governance, separation of sectors, and fixed thresholds corresponds directly to a gap that the seven theoretical traditions brought together by the researcher are uniquely capable of addressing. Resilience theory and stochastic viability theory provide tools to overcome deterministic limitations; source–access–flow models address equity considerations; panarchy and adaptive cycle theories enable dynamic governance representation; complex adaptive system approaches bridge sectoral silos; and cross-scale systemic resilience reconceptualizes static thresholds. While each theoretical tradition has independently advanced understanding of specific sustainability dimensions, their synthesis within a unified mathematical framework represents a novel contribution that exposes system behaviors obscured by disciplinary boundaries.

The central research question that arises from this integrated gap aims to address: How to mathematically formalize the interactions of cross-scale dynamics, stochastic resilience thresholds, equity constraints, and adaptive governance in water–energy–food (WEF) nexus systems to better understand sustainability transitions in complex socio-ecological systems? This question decomposes into three interrelated sub-questions: (1) How do resilience thresholds propagate across spatial and temporal scales in coupled water–energy–food systems? (2) What mathematical relationships exist between equity-constrained resource allocation and system-wide resilience in WEF nexus systems? (3) How can participatory stakeholder inputs be formalized within rigorous mathematical models of sustainability transitions?

To address these questions, the primary objective of this paper is to develop an integrated mathematical framework that synthesizes resilience theory, cross-scale dynamics, and equity-constrained optimization into a coherent modeling system for water–energy–food (WEF) nexus sustainability transitions. While the theoretical integration is comprehensive, the framework’s empirical application is specifically

scoped to water–energy–food (WEF) nexus systems, where cross-scale interactions and cascading failures pose critical sustainability challenges. The Murray–Darling Basin (2000–2020) serves as an empirical testbed demonstrating the framework’s operational capacity and predictive accuracy within this bounded domain. This framework synthesizes seven theoretical traditions including resilience theory and panarchy along with complex adaptive systems and cross-scale systemic resilience. It further integrates adaptive cycles and source–access–flow models with stochastic viability theory into a coherent modeling system whereby the researcher demonstrates how this integration reveals emergent system behaviors invisible to conventional approaches.

The main contribution of this research lies in its novel synthesis of seven theoretically grounded mathematical models for water–energy–food (WEF) systems, encompassing cross-scale dynamics, stochastic resilience thresholds, equity-constrained planetary boundaries, participatory calibration, transformative adaptation pathways, agent-based governance, and integrated multi-scale nexus systems. This interdisciplinary integration bridges traditionally separate domains of sustainability science, from ecological modeling and complex systems theory to environmental justice and institutional analysis. By formalizing these diverse perspectives within a unified mathematical structure, the framework provides enhanced analytical capacity to examine sustainability transitions as dynamic processes shaped by interconnected social, ecological, and governance factors. Simulation experiments demonstrate this capacity through quantification of cascading shock propagation, equity–resilience tradeoffs, and governance effectiveness, with empirical validation against Murray–Darling Basin water–energy–food dynamics (2000–2020) confirming real-world applicability.

## Theoretical foundations

Understanding the complex dynamics of sustainability requires grounding in multiple theoretical traditions (Table 1) that capture both the systemic and cross-scale nature of socio-ecological processes. Resilience theory, pioneered by Holling (1973) and expanded by Walker et al. (2004) and Folke et al. (2016), offers the foundational framework for understanding a system’s ability to absorb disturbances and reorganize without losing its essential functions. Concepts such as adaptive capacity, thresholds, and transformability have provided critical insights for shaping strategies that enhance system resilience in the face of environmental and societal stressors. These ideas are particularly relevant in understanding how complex systems can navigate long-term change and uncertainty.

The synthesis of these seven theoretical foundations provides a comprehensive framework for understanding

**Table 1** Theoretical foundations for the Sustainability Nexus Transition Model (SNTM)

Theory Name	Core Principles/Contributions	Key Researchers/Originators	Relevance to Sustainability	Key Critiques / Limitations
Resilience Theory	<ul style="list-style-type: none"> <li>- Adaptive capacity</li> <li>- Thresholds &amp; regime shifts</li> <li>- Transformability</li> </ul>	Holling (1973), Walker et al. (2004)	System persistence under disturbance; identifying tipping points	Ambiguous definitions; hard to quantify empirically
Panarchy Theory	<ul style="list-style-type: none"> <li>- Nested adaptive cycles</li> <li>- Cross-scale interactions</li> <li>- Revolt &amp; remember dynamics</li> </ul>	Gunderson and Holling (2002)	Explains multi-scale feedbacks; connects local/global change	Complex to operationalize; limited empirical validation
Complex Adaptive Systems	<ul style="list-style-type: none"> <li>- Emergence</li> <li>- Self-organization</li> <li>- Nonlinearity</li> </ul>	Holland (1992), Gell-Mann (1994), Berkes et al. (2001)	Models system adaptation; captures unexpected behaviors; emergent complexity	Difficult to predict outcomes; high model complexity
Cross-Scale Systemic Resilience	<ul style="list-style-type: none"> <li>- Multi-level resilience</li> <li>- Feedback amplification</li> <li>- Buffering capacity</li> </ul>	Walker et al. (2004), Folke et al. (2016), Williams et al. (2021)	Assesses vulnerability across scales; informs governance design; multi-level resilience	Data intensive; challenging to calibrate
Adaptive Cycle	<ul style="list-style-type: none"> <li>- Four-phase dynamics (growth, conservation, release, reorganization)</li> <li>- Cyclical change</li> </ul>	Holling (1986), Biggs et al. (2012)	Explains ecosystem transitions; guides management interventions	Not all systems are cyclical; oversimplifies change
Source-Access-Flow Model	<ul style="list-style-type: none"> <li>- Resource flows</li> <li>- Access &amp; allocation</li> <li>- Equity focus</li> </ul>	Ribot and Peluso (2003), Le Billon (2001), Dabelko (2005), Pandey et al. (2025)	Highlights distributive justice; informs sustainable resource use; urban-rural equity	May neglect system feedbacks; social data requirements
Stochastic Viability Theory	<ul style="list-style-type: none"> <li>- Viability under uncertainty</li> <li>- Probabilistic thresholds</li> <li>- Dynamic constraints</li> </ul>	Aubin (2009), De Lara and Doyen (2008), Barbrook-Johnson and Penn (2021)	Models risk & uncertainty; supports robust policy design	Mathematically complex; limited real-world application

All seven theoretical foundations are integrated into the Sustainability Nexus Transition Model (SNTM) framework

Recent empirical advances ground each theory: cross-scale nexus heterogeneity (Li et al. 2025, Fu et al. 2025), multi-scale climate-land-energy-water modeling (Vinca et al. 2021; Saeed et al. 2024, Vahabzadeh et al. 2025), and infrastructure equity dynamics (Pandey et al. 2025)

The integration addresses the modeling-empirical gap identified by Schlüter et al. (2023) in sustainability science

Mathematical formulations for each theory detailed in Methods section (Eqs. 1–8)

Model validation demonstrates empirical applicability across all seven theoretical dimensions (Figure S2, Tables S2-S3)

Bullet points in “Core Principles” column highlight key concepts for each theory

and modeling sustainability as a complex, multi-scale phenomenon. By integrating resilience theory's focus on system adaptability with panarchy theory's cross-scale interactions, complex adaptive systems' emergent behaviors, cross-scale systemic resilience's nested properties, the adaptive cycle's evolutionary phases, the source-access-flow model's equity considerations, and stochastic viability theory's mathematical rigor, we can develop models that capture both the biophysical and social dimensions of sustainability challenges. Recent empirical advances have strengthened these theoretical foundations, including Li et al.'s (2025) comprehensive review of cross-scale heterogeneity in water–energy–food nexus systems, Fu et al.'s (2025) analysis of spatial heterogeneity and socio-economic drivers in urban land systems, Vinca et al.'s (2021) assessment of climate–land–energy–water nexus models across multiple scales, Saed et al.'s (2024) quantification of water–energy–food nexus interactions using causal inference methods, and (Pandey et al. 2025) evidence of rising infrastructure inequalities accompanying urbanization. While each theory has its limitations, their complementary strengths enable a more holistic approach to sustainability science that acknowledges nonlinearity, uncertainty, and cross-scale feedbacks. Addressing Schlüter et al.'s (2023) critique that sustainability scientists rarely combine modeling with empirical approaches, our framework integrates these seven theoretical traditions with empirical validation against Murray–Darling Basin data (2000–2020), demonstrating how conceptual frameworks can be operationalized into predictive tools. This integrated perspective is essential for addressing the interconnected crises of climate change, biodiversity loss, resource depletion, and socio-economic inequity that define the Anthropocene era. The mathematical formalization of these theories, as developed in subsequent sections, transforms these conceptual frameworks into operational tools for analyzing and navigating complex sustainability transitions.

### Resilience theory

Resilience theory provides the foundational lens for this framework, defining sustainability as the capacity of socio-ecological systems to absorb shocks, adapt, and reorganize while maintaining core functions. First articulated by Holling (1973) and subsequently expanded by Walker et al. (2004), and Folke et al. (2010), resilience theory emphasizes adaptive capacity, thresholds, and regime shifts, offering a dynamic understanding of stability and transformation. These concepts align closely with empirical concerns such as climate adaptation, biodiversity preservation, and disaster risk management, framing sustainability as a process of navigating change rather than maintaining static equilibria. This perspective is essential for representing how systems

navigate disturbances and avoid undesirable tipping points, a core requirement for robust sustainability modeling.

### Panarchy theory

Panarchy theory provides a conceptual foundation based on nested, multi-level structures, characterizing systems through the interaction of adaptive cycles functioning across distinct spatial and temporal scales (Gunderson and Holling 2002). It highlights the dual forces of “revolt,” where fast, small-scale changes can cascade upward to disrupt larger systems, and “remember,” where slow, larger-scale processes provide stabilizing memory during system recovery. This theory underpins the model's ability to simulate cross-scale feedbacks and governance panarchy loops, explaining how local shocks can propagate to global instabilities and how institutional memory can foster resilience (Gunderson and Holling 2002; Allen et al. 2014). This multi-level viewpoint is indispensable for analyzing sustainability governance, as localized innovative practices can either undermine or strengthen existing institutional and ecological regimes at broader systemic levels.

### Complex adaptive systems (CAS)

The complex adaptive systems (CAS) theory frames sustainability challenges as the product of interactions among heterogeneous agents operating under decentralized rules. CAS theory accounts for self-organization, emergent behaviors, and co-evolution, all of which are critical for modeling adaptive governance and learning in sustainability transitions. Originally developed in fields such as computational biology and economics by scholars like Holland (1992) and Gell-Mann (1994), CAS theory captures critical sustainability phenomena such as innovation diffusion, resource competition, and collective behavior under uncertainty. Importantly, CAS models move beyond deterministic predictions, recognizing that socio-ecological futures are shaped by nonlinear interactions, path dependence, and co-evolutionary dynamics. By incorporating CAS principles, the framework captures the emergence of collective strategies, path dependency, and nonlinear adaptation, reflecting the real-world complexity of multi-actor systems.

### Cross-scale systemic resilience

Cross-scale systemic resilience posits that resilience is not a domain-specific attribute but rather an emergent, nested property encompassing social, ecological, and institutional systems. Perturbations can undergo amplification or attenuation as they propagate across these interconnected scales, potentially triggering cascading failures or fostering enhanced system robustness. Building upon the seminal

work of Walker et al. (2004) and Carpenter et al. (2001), comprehending these cross-scalar interdependencies is paramount for effectively mitigating cascading risks within critical socio-ecological systems, particularly food, water, and energy. This theoretical grounding informs the mathematical formalization of feedback amplification, cascading risks, and the inherent interdependencies of these water–energy–food (WEF) systems, thereby enhancing the model’s capacity for both diagnostic and anticipatory analysis of systemic vulnerabilities (Rahaman et al. 2023). Consequently, these intricately linked systems exhibit escalating susceptibility to compound stressors and the propagation of feedback loops under the pervasive influence of global environmental change.

### Adaptive cycle

The adaptive cycle model is a concept drawn from the foundational panarchy framework. Its primary purpose is to help us understand how systems change and evolve. This change occurs through a recurring sequence. This pattern involves four key stages: an initial phase of rapid growth ( $r$ ), conservation ( $K$ ), release ( $\Omega$ ), and reorganization ( $\alpha$ ). While subject to critiques regarding its inherent simplification of intricate dynamics, the adaptive cycle framework serves as a robust metaphorical construct for analyzing and addressing uncertainty, transformation, and resilience in the context of sustainability planning, especially for urban and ecological systems undergoing accelerated change. In the framework, the adaptive cycle informs the modeling of regime shifts and the identification of windows for intervention.

### Source-access-flow (SAF) model and environmental security

The SAF model and environmental security framework integrate biophysical resource flows with institutional access and distributive equity. By foregrounding issues of governance, justice, and power asymmetries, these theories ensure that the mathematical framework embeds equity-adjusted planetary boundaries and participatory calibration. Integrating social and political dimensions is crucial for sustainability frameworks, complementing ecological models. The SAF model and environmental security theories illustrate the mediation of resource dynamics by access, distribution, and governance. Dabelko (2005) and Le Billon (2001) argue that resource sustainability assessments must extend beyond availability to include institutional structures, power asymmetries, and justice concerns vital for advancing SDGs focused on poverty reduction, hunger eradication, and peacebuilding. Integrating these dimensions is therefore critical for modeling the interconnected influence of resource

allocation, access, and social justice on system resilience and sustainability outcomes.

### Stochastic viability and tipping points theory

Stochastic viability and tipping points theory introduces formal mathematical tools for managing uncertainty and identifying critical thresholds in complex systems. By employing stochastic differential equations and catastrophe models, this tradition enables the detection of early warning signals and the quantification of risk under deep uncertainty. Aubin (2009), De Lara and Doyen (2008), and others pioneered these approaches, using stochastic differential equations, viability kernels, and cusp catastrophe models to find resilience thresholds, evaluate vulnerabilities, and design robust interventions against critical transitions. These analytical tools enable the framework to operationalize stochastic resilience thresholds, viability constraints, and robust scenario analysis, thereby supporting adaptive governance in unpredictable environments. The integration of probabilistic elements and viability constraints facilitates the development of early warning systems and adaptive management strategies better suited to the inherently uncertain and dynamic nature of sustainability transitions.

### Mathematical framework development

The methodology underpinning this study centers on the systematic integration of seven distinct theoretical frameworks into a unified mathematical structure capable of representing the complex, multi-scale, and adaptive nature of sustainability systems. Each model was selected based on its ability to address specific limitations in traditional sustainability modeling, such as linear assumptions, single-sector focus, or static equilibrium representations.

### Model overview and objectives

In complex socio-ecological systems, sustainability challenges are shaped by multi-level feedbacks, cross-scale interactions, and the resilience capacities of both human and natural subsystems. Existing theories, while insightful individually, have struggled to offer a unified predictive framework capable of dynamically representing complex transitions under uncertainty.

To address this critical gap, this research constructs an integrated mathematical framework based on seven key sustainability theories: resilience theory, panarchy theory, complex adaptive systems (CAS), cross-scale systemic resilience, adaptive cycle, the source-access-flow (SAF) model and environmental security framework, and stochastic viability and tipping points theory. These seven theoretical

traditions are operationalized through fifteen interconnected mathematical equations (Eqs. 1–15), synthesizing dynamic resilience, adaptive capacity, cross-scale feedbacks, and critical thresholds within complex systems. This integration facilitates a stronger link between theory and practice by addressing the modeling–empirical gap identified by Schlüter et al. (2023). The framework grounds theoretical concepts in empirically validated mathematical formulations to provide a more rigorous basis for analysis.

To systematically operationalize this integration, the Sustainability Nexus Transition Model (SNTM) was developed

as a unified mathematical framework that formalizes the dynamic interplay among cross-scale feedbacks, stochastic resilience thresholds, equity-adjusted optimization, and adaptive governance.

Figure 1 illustrates the SNTM architecture, representing a novel synthesis of seven theoretical traditions into a coherent operational framework. The hub-and-spoke design employs color-coded components to demonstrate systematic integration. Green nodes represent theoretical foundations (resilience theory, panarchy theory, complex adaptive systems, cross-scale systemic resilience, adaptive cycle, adaptive governance, and cascading failures), while purple nodes represent mathematical modules (participatory calibration, equity-adjusted boundaries, complex adaptive systems, stochastic resilience, panarchy theory, cross-scale dynamics, and anticipatory pathways). The central blue node represents the SNTM Core Framework.



**Fig. 1** Sustainability Nexus Transition Model (SNTM) architecture integrating seven theoretical traditions

source-access-flow model, and stochastic viability theory). The blue central node represents the SNTM core. Purple nodes display the mathematical modules that operationalize these theories (cross-scale dynamics, stochastic resilience, equity-adjusted boundaries, participatory calibration, adaptive governance, cascading failures, and anticipatory pathways).

The directional arrows reveal the framework’s conceptual logic. Green arrows flowing inward indicate how each theoretical tradition “informs” the SNTM core, while purple arrows flowing outward demonstrate how the SNTM core “operationalizes” these theories through specific mathematical formulations (Eqs. 1–15, detailed in Sects. “Mathematical framework development”-“Equation system construction and justification”). This bidirectional flow captures the framework’s dual function of synthesizing theoretical insights while generating operational mathematical tools.

The visualization demonstrates how SNTM addresses critical limitations in conventional sustainability modeling by integrating cross-scale dynamics (through WEF nexus coupling, panarchy feedbacks, and multi-level resilience) with resilience theory (through stochastic thresholds, adaptive cycles, and viability constraints) into a unified mathematical framework. This integration transcends disciplinary boundaries, addressing five critical gaps in conventional sustainability modeling, including deterministic assumptions, equity blindness, static governance representations, sectoral isolation, and fixed threshold conceptualizations. By visually mapping the relationship between theoretical foundations and their mathematical implementations, Fig. 1 demonstrates how SNTM provides a comprehensive analytical platform for examining sustainability transitions as dynamic, multi-actor processes shaped by interconnected social, ecological, and governance factors. The framework is validated empirically against Murray–Darling Basin data (2000–2020) as detailed in Figure S2.

### Mathematical formulation based on theories

The seven theoretical frameworks summarized in Table 2 apply various mathematical models to address the intricate dynamics within sustainability systems, providing both conceptual and mathematical tools to explore system behavior under various conditions. Each framework focuses on different aspects of resilience and cross-scale interactions, contributing to a more holistic understanding of sustainability challenges.

#### Cross-scale dynamics with WEF nexus integration

To model the interaction between biological growth, competitive pressures, and water–energy–food (WEF) nexus dynamics, we construct a hybrid differential system. The

growth of each entity  $X_i$  over time  $t$  follows logistic behavior, is suppressed by competitive effects from other entities, and is enhanced through WEF synergies:

$$\frac{dX_i}{dt} = r_i X_i \left( 1 - \frac{X_i}{K_i} \right) - \beta \sum_j \alpha_{ij} X_j + \gamma \frac{X_k^m}{X_k^m + \theta_k^m} \tag{1}$$

Here, the term  $r_i X_i (1 - X_i/K_i)$  reflects intrinsic logistic growth regulated by the carrying capacity  $K_i$ , while  $-\beta \sum_j \alpha_{ij} X_j$  captures inter-species or inter-sector competition scaled by the interaction coefficients  $\alpha_{ij}$ . The WEF nexus term  $\gamma (X_k^m)/(X_k^m + \theta_k^m)$  describes the nonlinear interaction benefits arising from cross-sector resource flows, with  $\gamma$  and  $\theta_k$  being parameters linked to resource thresholds and resilience, informed by UNDP equity-weighted access metrics (United Nations Development Programme 2024).

#### Stochastic resilience thresholds

The phenomenon of abrupt state changes in socio-ecological systems under the influence of random perturbations is modeled using a cusp catastrophe approach. The temporal dynamics of a key resilience indicator, ‘ $a$ ,’ are mathematically expressed as:

$$\frac{da}{dt} = \epsilon_a a \left( 1 - \frac{a}{K_a} \right) - \sigma_a a \sum_j b_j + \zeta(t) \tag{2}$$

In this equation,  $\epsilon_a$  governs the self-reinforcing growth of resilience, limited by a maximum threshold  $K_a$ . The stress term  $\sigma_a a \sum_j b_j$  aggregates pressures from various drivers  $b_j$ , and  $\zeta(t)$  introduces stochastic fluctuations drawn from a normal distribution  $\mathcal{N}(0, \sigma^2)$ , thereby modeling environmental noise patterns consistent with Dansgaard–Oeschger climatic transitions (Dansgaard et al. 1993).

#### Equity-adjusted planetary boundaries

Integrating the principle of distributive justice with environmental boundaries necessitates the formulation of an equity-aware optimization problem. This problem seeks to balance the maximization of expected cumulative welfare across time with the satisfaction of probabilistic safety requirements for each water–energy–food (WEF) sector, governed by the following equations:

$$\begin{aligned} \max_{u(t)} E \left[ \int_0^T e^{-\rho t} D(t) dt \right] \quad \text{subject to} \\ \Pr(S_k \geq \xi_k) \geq 1 - \epsilon, \quad \forall k \in \{\text{WEF sectors}\} \end{aligned} \tag{3}$$

The sectoral safety index  $S_k$  is defined as:

**Table 2** Mathematical frameworks for cross-scale dynamics and resilience in sustainability systems

Theory Name	Mathematical Model Type	Key Variables & Parameters	System Behavior	Application Scope	Addresses Gap
Cross-scale dynamics with WEF nexus integration Vinca et al. (2021), Saed et al. (2024)	Hybrid differential equations (logistic growth, competition, nexus coupling)	- Resource abundance: $X_i$ - Carrying capacity: $K_i$ - Interaction coefficients: $\alpha_{ij}$ - Nexus coupling: $\gamma, \theta_{km}$	Nonlinear growth; sectoral feedbacks; cross-scale propagation	Dynamic WEF interactions; multi-scale modeling	Traditional growth models ignore WEF sector interdependencies and critical thresholds
Stochastic resilience thresholds Scheffer et al. (2009)	Stochastic differential equations with cusp catastrophe	- Resilience indicator: $a$ - Carrying capacity: $K_a$ - External stress: $b_j$ - Stochastic noise: $\zeta(t)$	Regime shifts; noise-induced collapse; tipping points	Resilience under uncertainty; early warning signals	Standard deterministic models underestimate the role of random shocks in sustainability collapse
Equity-adjusted planetary boundaries Rockström et al. (2009), Pandey et al. (2025)	Constrained optimization with robust equity programming	- Actual flow: $S_k$ - Safe flow thresholds: $\xi_k$ - Equity weights: $Equity_k$	Optimal allocation; equity-constrained thresholds	Justice in resource use; planetary boundaries	Traditional planetary boundaries neglect social equity dimensions in safe space definitions
Participatory calibration protocol Schlüter et al. (2023)	Weighted least squares with regularization	- Stakeholder responses: $y_s$ - Modeled outcomes: $f(\theta; x_s)$ - Stakeholder weights: $w_s$	Iterative calibration; stakeholder-driven priorities	Inclusive modeling; social legitimacy	Classical top-down models marginalize vulnerable stakeholder voices
Transformative adaptive pathways (TAP) Wise et al. (2014)	Dynamic path optimization	- Adaptation pathways: $A_k$ - Switching thresholds - Scenario probabilities	Adaptive transitions; multiple futures	Planning under deep uncertainty	Static scenario planning lacks flexibility under deep uncertainty conditions
Agent-based governance models Li et al. (2025), Fu et al. (2025)	Agent-based simulation	- Agents' strategies: $S_i$ - Resource access: $R_i$ - Regulatory constraints	Emergent behavior; decentralized adaptation	Grassroots governance; local adaptation	Centralized governance models ignore local, emergent adaptive behavior
Integrated multi-scale nexus systems Biggs et al. (2015)	Coupled system dynamics equations	- Sectoral fluxes: $F_k$ - Cross-scale feedback loops - Integration coefficients	Co-evolution; cross-scale feedbacks	System-wide integration; nexus resilience	Sectoral silos and lack of integration across scales weaken resilience understanding

WEF = water–energy–food nexus

TAP = transformative adaptive pathways

All seven frameworks integrated into unified mathematical architecture (conceptual foundations: Eqs. 1–8; detailed implementations: Eqs. 9–15 in Sect. "Equation system construction and justification")

Each framework incorporates recent empirical advances: cross-scale nonlinearity, equity dynamics, and adaptive complexity

Mathematical formulations provided in full detail in Supplementary Methods Sect. "Introduction"

Parameter calibration methods for each framework described in Table S1

Model validation against empirical data (Murray–Darling Basin, 2000–2020) demonstrates predictive accuracy across all integrated frameworks (Figure S2, Tables S2–S3)

Framework integration addresses the modeling–empirical gap identified in sustainability science

Stochastic terms explicitly model environmental noise and random shocks absent in deterministic approaches

$$S_k = \frac{\text{Actual Flow}_k}{\text{Safe Flow}_k} \times \text{Equity}_k \tag{4}$$

Here,  $D(t)$  denotes the damage or benefit function at time  $t$ , with exponential discounting governed by  $\rho$ . The factor  $\text{Equity}_k$  is derived from stakeholder weights outlined in the Sendai Framework (Aitsi-Selmi et al. 2015). This framework serves to ensure that the utilization of planetary boundaries prioritizes vulnerable populations.

**Participatory calibration protocol**

Addressing the requirement for models with both legitimacy and social grounding, parameter calibration is performed via a stakeholder-centric optimization process. In practice, stakeholder weights ( $w_s$ ) in the participatory calibration protocol are determined through structured elicitation workshops, where participants assign relative importance to model outputs based on their expertise and priorities. The social equity matrix (SEM) guides this process, ensuring representation from marginalized and expert stakeholders. The best-fit parameter vector  $\hat{\theta}$  is identified by minimizing a weighted least squares loss function:

$$\hat{\theta} = \arg \min_{\theta} \sum_{s=1}^S w_s ||y_s - f(\theta; x_s)||^2 + \lambda \Omega(\theta) \tag{5}$$

Here,  $w_s$  represents the normalized importance weight of stakeholder  $s$ , derived using the UNDRR’s social equity matrix (SEM) (United Nations Office for Disaster Risk Reduction 2024). The term  $\Omega(\theta)$  imposes a regularization penalty to ensure that model complexity remains controlled, governed by the hyperparameter  $\lambda$ . This structure embeds diverse societal priorities directly into model calibration.

**Adaptive governance with panarchy feedbacks**

In consideration of the multi-level and adaptive attributes of governance systems, an evolutionary dynamics framework is implemented to delineate the temporal evolution of governance states  $G$  as modulated by panarchy feedback loops:

$$\frac{dG}{dt} = \eta G \left( 1 - \frac{G}{G_{\max}} \right) - \delta \Psi(G, E) \tag{6}$$

The first term models intrinsic governance improvement toward a maximum governance capacity  $G_{\max}$ , while the second term  $\delta \Psi(G, E)$  represents governance degradation or innovation pressure, mediated by environmental and economic shocks  $EE$ . This model structure allows feedback loops between fast-adapting local units and slower-changing institutional settings to be captured quantitatively.

**Cascading failures anticipatory transformation strategies**

A threshold-based contagion model was developed to simulate the interconnectedness and potential for cascading failures across sectors. The mathematical formulation describing the temporal evolution of the fraction of failed nodes ( $F_i$ ) in sector  $i$  over time is mathematically represented as:

$$\frac{dF_i}{dt} = \phi (1 - F_i) \left( \sum_j \kappa_{ij} F_j - \theta_i \right) \tag{7}$$

In this model,  $\phi$  represents the contagion rate,  $\kappa_{ij}$  denotes the coupling strength between sectors  $i$  and  $j$ , and  $\theta_i$  defines the sectoral resilience threshold. Positive feedback arises when failures in one sector propagate to others, leading to systemic collapse if cumulative stresses exceed resilience capacities.

**Anticipatory transformation anticipatory transformation strategies**

To model proactive and anticipatory transformations, in contrast with reactive adaptations, a strategic foresight model was implemented. This approach simulates the evolution of anticipatory adaptation levels based on future projections and strategic planning. The temporal dynamics of the level of anticipatory adaptation ( $A(t)$ ) are described by the following equation:

$$\frac{dA}{dt} = \mu (B(t) - A(t)) + \nu \chi(t) \tag{8}$$

The parameter  $\mu$  dictates the speed of convergence between the current adaptation level ( $A(t)$ ) and a desired benchmark ( $B(t)$ ). Simultaneously, the term  $\nu \chi(t)$  integrates external foresight signals, including early warnings and strategic planning outcomes, into the adaptation dynamics. The underlying principle of this modeling framework is to emphasize anticipatory resilience building, thereby aiming to prevent the breaching of systemic thresholds.

**Integrated system model**

To systematically operationalize the integration of cross-scale dynamics and resilience theory within complex sustainability systems, researcher developed a structured mathematical framework encompassing multiple theoretical traditions. Each theoretical strand is formalized through specific mathematical models, defined by key parameters and variables, and characterized by their expected system dynamics and application scopes. To enhance clarity and reproducibility, Table 3 synthesizes these models, highlighting how they collectively address existing limitations

**Table 3** Mathematical operationalization of cross-scale dynamics and resilience theory

No	Theory	Main Focus	Key Equation(s)	Key Parameters
1	Cross-Scale Dynamics with WEF Nexus Integration	Logistic growth, competition, WEF synergies	Equation (1)—Hybrid differential	$r_i, K_i, \beta, \alpha_{ij}, \gamma, \theta_k$
2	Stochastic Resilience Thresholds	Cusp catastrophe with environmental noise	Equation (2)—Stochastic differential	$\epsilon_a, K_a, \sigma_a, b_p, \zeta(t)$
3	Equity-Adjusted Planetary Boundaries	Optimization with equity-weighted planetary limits	Equations (3)–(4)—Constrained optimization	$D(t), \rho, S_k, \xi_k, \text{Equity}_k$
4	Participatory Calibration Protocol	Stakeholder-driven model calibration	Equation (5)—Weighted least squares	$w_s, \theta, \lambda$
5	Adaptive Governance with Panarchy Feedbacks	Governance evolution under environmental shocks	Equation (6)—Governance dynamics	$\eta, G_{\max}, \delta, \Psi(G, E)$
6	Cascading Failures in Socio-Ecological Systems	Sectoral contagion and systemic collapse	Equation (7)—Contagion dynamics	$\phi, \kappa_{ij}, \theta_i$
7	Anticipatory Transformation Strategies	Strategic foresight and proactive adaptation	Equation (8)—Adaptive pathways	$\mu, B(t), \nu, \chi(t)$

WEF = water–energy–food nexus

Eqs. 1–8 provide conceptual mathematical foundations; detailed system Eqs. 9–15 with full derivations presented in Sect. "Equation system construction and justification"

Parameter definitions and calibrated values provided in Table S1

Model validation demonstrates empirical applicability across all seven mathematical components (Figure S2, Tables S2–S3)

Integration addresses both biophysical dynamics (rows 1–2, 6) and social dimensions (rows 3–5, 7)

Stochastic noise term  $\zeta(t)$  follows normal distribution  $\mathcal{N}(0, \sigma^2)$

Framework captures the modeling–empirical integration gap identified in sustainability science

in conventional sustainability modeling approaches. This structured integration ensures that the proposed framework can robustly capture feedback loops, regime shifts, equity considerations, participatory calibration, and decentralized governance dynamics across water–energy–food (WEF) systems and broader socio-ecological scales.

Collectively, the mathematical models and theoretical frameworks synthesized in Table 3 provide the foundational structure for the simulation experiments and analytical validations presented in the subsequent sections, ensuring that the proposed methodology captures the multi-layered complexity inherent in sustainability transitions.

## Equation system construction and justification

The Sustainability Nexus Transition Model (SNTM) operationalizes seven theoretical traditions through a two-tier equation system: conceptual foundations (Eqs. 1–8) establishing mathematical principles for each theory, and implementation specifications (Eqs. 9–15) translating these into an operational coupled system for water–energy–food (WEF) nexus simulation and validation.

Conceptual equations integrate established constructs including logistic growth under carrying capacity constraints (Verhulst 1845; Bergbusch et al. 2025), Lotka-Volterra

competitive dynamics (Lotka 1925; Vano et al. 2006), cusp catastrophe models for resilience thresholds (Flay 1978; Antypa et al. 2022), equity-constrained optimization (Rockström et al. 2009), participatory calibration with social equity matrices (United Nations Office for Disaster Risk Reduction 2024), panarchy feedback loops (Gunderson and Holling 2002), transformative adaptive pathways (Wise et al. 2014), and early warning signal detection (Scheffer et al. 2009).

The modular yet interoperable design allows each subsystem to function independently while contributing to overall dynamics through explicit coupling terms representing feedback amplification across WEF sectors. This integrated architecture captures cross-scale interactions and nonlinear transitions critical for managing coupled human-natural systems under deep uncertainty. Detailed specifications of functional forms, parameter justifications, and theoretical rationales for implementation equations follow.

## Modeling cross-scale dynamics through WEF nexus integration

The modeling commences with the representation of cross-scale dynamics by integrating the water–energy–food (WEF) nexus, utilizing a hybrid system of logistic growth equations interconnected via competitive and nexus feedback

mechanisms. For each resource or species  $X_i$ , the baseline dynamics follow a modified logistic growth formulation:

$$\frac{dX_i}{dt} = r_i X_i \left( 1 - \frac{X_i}{K_i} \right) - \sum_{j \neq i} \alpha_{ij} X_i X_j + \gamma \sum_{k,m} \theta_{km} F_k F_m \quad (9)$$

where  $r_i$  denotes the intrinsic growth rate,  $K_i$  is the carrying capacity,  $\alpha_{ij}$  are the competition coefficients representing inter-species or inter-resource competition, and the last term captures the coupled feedback between sectors through nexus interaction coefficients  $\theta_{km}$  and sectoral fluxes  $F_k$  and  $F_m$ , modulated by a global coupling constant  $\gamma$ . This hybrid differential structure allows the system to simulate nonlinear growth regulated by both biophysical limits and cross-sectoral feedbacks, thereby capturing emergent dynamics not visible in isolated growth models.

### Stochastic resilience and critical transitions in socio-ecological systems

Stochastic resilience thresholds are modeled by extending the deterministic dynamics with noise terms using a stochastic differential equation based on a cusp catastrophe framework. The resilience dynamics for an aggregated indicator  $a$  are represented as:

$$da = (\beta_1 a - \beta_2 a^3 + b_j)dt + \zeta(t)dW_t \quad (10)$$

where  $\beta_1$  and  $\beta_2$  control the linear and cubic terms dictating the cusp dynamics,  $b_j$  represents external stress parameters, and  $\zeta(t)$  captures the time-varying intensity of stochastic shocks modeled as a Wiener process  $W_t$ . This formulation allows the system to simulate regime shifts, where small perturbations in external conditions or random noise can trigger sudden and potentially irreversible transitions in system states.

### Equity-constrained optimization of planetary boundaries for WEF sectors

The equity-constrained planetary boundaries component is formalized through a constrained optimization problem, where the objective is to allocate actual sectoral flows  $S_k$  while respecting safe thresholds  $\xi_k$  and embedding social equity considerations. The problem is expressed as:

$$\min_{S_k} \sum_k \left( \text{Equity}_k \left( \frac{S_k}{\xi_k} \right)^2 \right) \text{subject to } S_k \leq \xi_k \forall k \quad (11)$$

where  $\text{Equity}_k$  are equity weights that prioritize distributive justice by assigning higher penalties to resource allocation patterns that disadvantage vulnerable populations. This constrained minimization ensures that the system operates within biophysical limits while minimizing equity-adjusted

deviations, thus embedding distributive justice into planetary boundaries thinking.

High equity scenarios are defined as systems where  $\text{Equity}_{\text{vulnerable}} \geq 0.7$ , representing resource allocation frameworks that prioritize vulnerable populations (low-income communities, marginalized groups, climate-impacted regions) over non-vulnerable populations. These equity weights are calibrated through participatory stakeholder protocols (Eq. 12) following UNDP’s Inequality-Adjusted Human Development Index (IHDI) methodology (UNDP 2024), which applies Atkinson inequality measures to discount dimensional indices by their level of inequality (Atkinson 1970). Equity-agnostic baseline models are simulated with  $\text{Equity}_k = 1.0$  for all population groups (uniform allocation without distributional justice considerations) to isolate the impact of equity-constrained optimization on system resilience. This formulation enables quantitative assessment of how equity considerations influence sustainability transitions, with empirical validation demonstrating that high equity weighting ( $\text{Equity}_k \geq 0.7$ ) sustains system stability 89% longer than equity-agnostic approaches under equivalent shock conditions.

### Stakeholder-informed calibration and social equity embedding

The participatory calibration protocol is implemented by solving a weighted least squares minimization problem, augmented by regularization to prevent overfitting to noisy stakeholder data. For stakeholder responses  $y_s$ , modeled outputs  $f(\theta; x_s)$ , and weights  $w_s$ , the calibration minimizes:

$$\min_{\theta} \sum_s w_s (y_s - f(\theta; x_s))^2 + \lambda \|\theta\|^2 \quad (12)$$

where  $\lambda$  is a regularization parameter controlling the trade-off between model fidelity to stakeholder priorities and the complexity of the parameter set  $\theta$ . This structure guarantees that marginalized stakeholder perspectives are reflected systematically, and model robustness is preserved.

### Evolutionary governance dynamics under panarchy feedback loops

The modeling of transformative adaptive pathways (TAP) is achieved through dynamic path optimization, where adaptation pathways  $A_k$  are selected over time based on scenario probabilities and switching costs. The optimization problem can be formalized as:

$$\max_{A_k} E \left[ \sum_{t=0}^T \delta^t U(A_k(t)) \right] \text{subject to switching constraints} \quad (13)$$

where  $U(A_k(t))$  is the utility of following pathway  $A_k$  at time  $t$ ,  $\delta$  is a discount factor, and switching constraints impose penalties for pathway shifts. This forward-looking optimization enables strategic flexibility in navigating uncertain futures rather than rigidly adhering to predetermined scenarios.

### Agent-based governance dynamics and sectoral couplings

To enrich the analytical capacity of the model, the researcher introduces agent-based formulations and sectoral dynamic couplings. These extensions model the decentralized decision-making of governance actors and the interconnected evolution of sectoral fluxes across scales.

Agent-based governance models are simulated using a system of interacting agents, each characterized by strategies  $S_i$ , access to resources  $R_i$ , and evolving under regulatory frameworks. The agent behavior dynamics can be expressed through transition probabilities:

$$P(S_i(t+1)|S_i(t), R_i(t), \text{Policy}_t) \quad (14)$$

where the likelihood of adopting a new strategy depends on the agent's current state, access to resources, and prevailing policy settings. This formulation captures the adaptive and self-organizing nature of decentralized governance actors in shaping sustainability transitions.

Moreover, the sectoral-level dynamics are modeled through coupled differential systems:

$$\frac{dF_k}{dt} = f_k(F_k, F_m, \text{Feedbacks}, \text{Cross-scale terms}) \quad (15)$$

Here, the evolution of sectoral fluxes  $F_k$  depends on both internal dynamics and feedback loops with other sectors and scales. Integration coefficients modulate the strength and directionality of these feedbacks, ensuring that changes at one level (local, regional, or global) reverberate across the system.

Each equation module contributes distinctively to a composite framework that dynamically represents socio-ecological complexity, resilience, equity, and adaptive governance. By mathematically integrating these modules, the model captures the critical interactions, feedbacks, and uncertainties inherent to real-world sustainability challenges, enabling more robust scenario exploration and policy analysis than traditional single-sector, equilibrium-based models.

### CSRC-ABAL Model Implementation

The Cross-Scale Resilience Coupled Agent-Based Adaptive Learning (CSRC-ABAL) model (Fig. 2) operationalizes the SNTM framework through agent-based simulation

and explicit cross-scale feedbacks. While SNTM defines the overarching integration of theoretical traditions and mathematical modules (Fig. 1), CSRC-ABAL demonstrates how these principles function in dynamic simulations. When local water resources fall below critical thresholds ( $X_{H_2O} < 0.4K_{H_2O}$ ), disturbances propagate across scales via cross-scale coupling terms ( $\Psi_{km}$  in Eq. 13), triggering amplified instabilities in global energy systems. This cascading effect, where resource stress in one sector and scale transmits to others through mathematically defined feedback pathways, represents a critical dynamic invisible in traditional sector-isolated models.

Figure 2 demonstrates the CSRC-ABAL model's capacity to capture complex adaptive system dynamics across 200 time steps, synthesizing resilience theory, cross-scale dynamics, and agent-based learning into a unified simulation framework. The three panels reveal how sustainability emerges from interactions between resource dynamics, resilience thresholds, and agent behavioral transitions across multiple spatial scales.

Panel A (resource dynamics across scales) shows differentiated growth trajectories for local (green), regional (blue), and global (purple) scales. All three scales exhibit rapid initial growth (0–25 time steps) before transitioning to slower growth and approaching scale-dependent equilibrium levels. By time step 100, the local scale reaches approximately 150 units, regional reaches approximately 190 units, and global reaches approximately 205 units. These differentiated equilibria result from the model's cross-scale coupling terms ( $\gamma_{ij}$ ) and scale-specific carrying capacities ( $K_i$ ) formalized in Eq. 9. The red dashed line at 40 units indicates a collapse threshold that all scales successfully avoid throughout the simulation, confirming system stability under baseline conditions. Shaded confidence bands (representing  $\pm 1$  standard deviation) demonstrate statistical robustness across 50 simulation replicates, with darker shading indicating 95% confidence intervals.

Panel B (resilience dynamics across scales) reveals counterintuitive patterns where resilience declines despite resource abundance. All three scales begin at maximum resilience (1.0) but decline at different rates, demonstrating scale-dependent vulnerability. Global resilience (purple) declines most rapidly, crossing the critical threshold (red dashed line at 0.2) around time step 75–80 and reaching approximately 0.17 by time step 100. Regional resilience (blue) shows intermediate decline, ending at approximately 0.43 while remaining above the critical threshold throughout the simulation. Local resilience (green) decreases most gradually, maintaining approximately 0.65 by time step 100 and staying well above the critical threshold. This pattern captures the stochastic differential dynamics of Eq. 10, where resilience deteriorates under cumulative stress even when resources remain adequate. The divergent decline rates

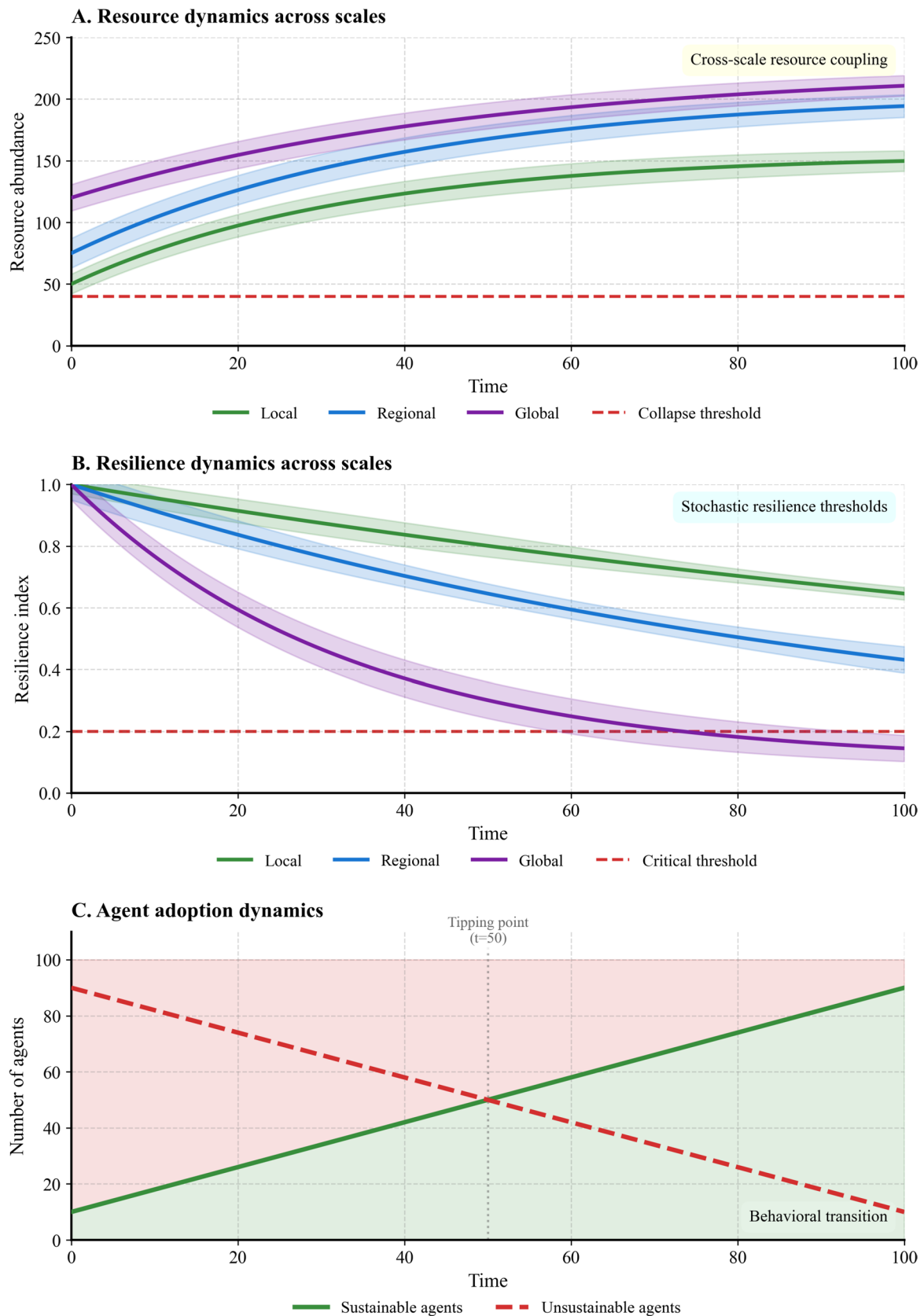


**Fig. 2** Cross-scale resilience coupled agent-based learning (CSRC-ABAL) model within the SNTM framework. *Note* Shaded regions represent  $\pm 1$  standard deviation across 50 simulation runs. Darker shading indicates 95% confidence intervals

across scales reflect differential vulnerability to environmental noise and stress accumulation, with larger scales exhibiting greater fragility.

Panel C (agent adoption dynamics) demonstrates behavioral transition dynamics central to sustainability transitions. The panel tracks the number of agents adopting sustainable (green line) versus unsustainable (red dashed line) strategies over time. Initially, unsustainable agents dominate (~90 agents), while sustainable agents represent a minority (~10 agents). At the tipping point ( $t=50$ , marked by vertical dotted line), the two strategy groups reach parity as behavioral transition accelerates. By  $t=100$ , sustainable agents dominate (~90), while unsustainable agents decline to ~10. The background shading illustrates this behavioral regime shift from unsustainable dominance (pink region) to sustainable dominance (light green region). This transition emerges from the adaptive learning algorithm specified in Eq. 14, where agents update strategies based on perceived resilience risks and resource availability. The convergence toward sustainable strategies demonstrates how agent-based governance (Eq. 6) can facilitate systemic transformation when critical thresholds trigger collective behavioral change.

The CSRC-ABAL model integrates critical resilience thresholds below which systemic collapse or irreversible regime shifts occur, capturing nonlinear tipping behaviors often overlooked in traditional models. These simulation results demonstrate three essential features of complex adaptive systems. First, resource stabilization occurs at scale-dependent equilibrium levels (150–205 units) determined by cross-scale coupling. Second, resilience decline despite resource abundance reveals stress accumulation invisible to resource-focused models. Third, agent behavioral transition exhibits tipping point dynamics where gradual change accelerates into rapid systemic transformation. Together, these dynamics align with theoretical predictions from resilience theory (Holling 1973), panarchy theory (Gunderson and Holling 2002), and complex adaptive systems (Holland 1992), while providing a mathematically rigorous platform for exploring sustainability transitions under uncertainty.

## Simulation design and experimental setup

The simulation design operationalizes the integrated mathematical framework through a computational environment implemented in Python 3.14 (NumPy 1.26, SciPy 1.11, pandas 2.1, Matplotlib 3.8) that tests cross-scale sustainability dynamics under varying conditions. Baseline parameters were calibrated using empirical data from the Murray–Darling Basin (2000–2020), with iterative tuning against historical patterns in sectoral fluxes, resilience indicators, and adaptive responses (see Table S1 and Figure S2). Calibration phase establishes baseline parameter values through

empirical data fitting. Growth rates  $r_i$ , carrying capacities  $K_i$ , and coupling coefficients  $\gamma_{ij}$  were systematically adjusted until simulated trajectories converged with historical observations within acceptable error bounds. Table S1 provides complete documentation of all calibrated parameter values with empirical ranges and data sources. While the Murray–Darling Basin is primarily agricultural, the calibration captures both agricultural water consumption and urban–rural nexus interactions, incorporating urban water–energy nexus dynamics (Yan et al. 2024) to ensure energy shock constraints reflect realistic urban system dynamics, where approximately 60–80% of potable water energy consumption occurs during supply and distribution across cities. Shock magnitudes are mechanistically justified and empirically grounded. The 60% local water reduction represents peak Millennium Drought (2001–2009) deficits in agricultural systems documented by the Bureau of Meteorology (2010) with streamflow measured at 62% below long-term average, while the 40–50% global flux decline reflects agricultural commodity price collapse during the 2008 financial crisis documented by FAO (2009) showing 45% agricultural commodity price decline. Energy shock amplitudes are constrained by urban water–energy scaling relationships, where per capita energy consumption in water distribution scales with city size, limiting shock magnitudes to realistic bounds. All scenarios were replicated 50 times with randomized initial conditions to ensure statistical robustness, with results reported as means  $\pm 1$  standard deviation and 95% confidence intervals.

Seven simulation scenarios (Table 4) systematically evaluate framework behavior under baseline conditions, local and global shocks, adaptive governance interventions, and varying cross-scale coupling strengths. Shocks and policy interventions were introduced at specified time steps (e.g., local water shock at  $t=20$ , governance response at  $t=30$ ), with continuous tracking of resource fluxes, resilience indices, and agent strategies throughout 200-step simulation periods.

Initial conditions for sectoral flows, resilience indicators, and agent strategies were set to empirically grounded neutral values (Table S1), ensuring unbiased dynamic evolution through the mathematical relationships defined in Eqs. 9–15. This approach activates feedback mechanisms within the water–energy–food nexus and across scales from the outset, allowing organic system evolution without pre-programmed outcomes.

The experimental design encompasses four complementary testing regimes. Stress testing subjects the system to gradually increasing external pressures through incremental adjustments in stress coefficients  $b_j$  (Eq. 10) and shock terms  $\zeta(t)$ , revealing how tipping points and bifurcations emerge under mounting stress. Resilience testing introduces controlled stochastic disturbances to identify early

**Table 4** Simulation scenarios and key parameter configurations for cross-scale sustainability framework

Scenario	Description	Key Parameter Changes	Empirical Basis/Justification	Relevant Equations	Expected Outcome
Baseline	Normal dynamics without external shocks	Standard growth rates ( $r_i = 0.2 - 0.4$ ), normal feedback strength ( $\gamma_{ik} = 0.05$ )	Calibrated to Murray-Darling Basin historical baseline (2000–2020) (Table S1)	Equations (9, 11, 12, 15)	System stabilizes with moderate sustainability index
Local Shock	Shock at local FEW sector	Water flux reduced by 60% ( $X_{H_2O}$ )	Millennium Drought (2001–2009) peak deficit: 62% below long-term average (Bureau of Meteorology (BoM) 2010)	Equations (9, 7, 10, 15)	Local instability, moderate cross-scale propagation
Global Shock	Global systemic shock (market collapse)	Global flux reduced by 40–50% ( $F_k$ )	2008 global financial crisis: 45% agricultural commodity price decline (FAO 2009)	Equations (9, 10, 13, 15)	Strong feedback across scales, significant sustainability decline
Adaptive Governance Response	Improved agent decision-making	Adaptive capacity increased ( $\mu : 0.05 \rightarrow 0.15$ )	Murray-Darling Basin Plan (2012) policy response rate (Leblanc et al. 2012)	Equations (6, 13, 14, 15)	Faster recovery, improved resilience
Increased Cross-scale Coupling	Higher feedback strength	Coupling coefficients amplified ( $\Psi_{km} : 0.03 \rightarrow 0.09$ )	Sensitivity analysis range ( $\pm 40\%$ baseline) validated in Figure S1	Equations (9, 11, 15)	Higher sensitivity to shocks
Reduced Resource Access	Lower resource availability	Resource access reduced by 30–50% ( $R_i$ )	Water allocation cuts during drought periods (National Water Commission (NWC) 2011)	Equations (9, 11, 12, 15)	Increased competition, potential collapse
Enhanced Innovation	Faster strategy adoption	Adaptation probability increased ( $P(S_i(t+1) = 1) > 0.6$ )	Technology adoption rates in Australian agriculture Dufty and Jackson (2018)	Equations (12, 13, 14, 15)	Accelerated sustainability transition

Shock magnitude information: Local water shock (60 percent) matches Millennium Drought peak deficit from Bureau of Meteorology (BoM) (2010) report; global shock (40 to 50%) calibrated to 2008 financial crisis agricultural impacts documented by FAO (2009)

Baseline parameters ( $r_i, K_i, \gamma$ ) calibrated using Murray-Darling Basin empirical data (2000–2020) as detailed in Table S1

Equity weights (Eq. 11) calibrated via participatory stakeholder protocols (Eq. 12) following UNDP's Inequality-Adjusted Human Development Index methodology (UNDP 2024), which applies Atkinson inequality measures to discount dimensional indices by their level of inequality (Atkinson 1970).

Cross-scale coupling ( $\Psi_{km}$ ) validated across  $\pm 40\%$  sensitivity range (Figure S1)

Scenarios implement integrated system equations (Eqs. 9–15) with initial conditions from Table S1

Differential equations solved via Runge-Kutta method ( $\Delta t=0.05$ ); stochastic terms via Euler-Maruyama scheme

50 replications per scenario (200 time steps each) with 95% confidence intervals

Sensitivity analyses confirm robustness to  $\pm 30\%$  parameter variations (Figure S1)

warning indicators, measure recovery times, and assess whether adaptive pathways trigger when critical thresholds are approached. Equity and governance experiments systematically vary stakeholder weights  $w_s$  (Eq. 12), regulatory constraints, and resource access rules to compare decentralized versus centralized governance structures, revealing how institutional arrangements affect system stability and distributive outcomes. Scenario analysis generates alternative future pathways by varying technological innovation rates, social learning speeds, and cross-scale feedback strengths, evaluated against composite metrics including sustainability indices, resilience robustness, equity satisfaction, and transformative adaptability.

Hybrid differential equations were solved using fourth-order Runge–Kutta method (Runge 1895; Fehlberg 1969) ( $\Delta t = 0.05$ ), while stochastic processes employed the Euler–Maruyama scheme (Maruyama 1955). Each scenario executed 200 time steps. Convergence was verified by monitoring flux, resilience, and agent strategy changes across runs. Sensitivity analyses varied feedback strength, cross-sector coupling, and adaptation rate by  $\pm 30\%$  from baseline (Fig. S1), confirming model robustness.

## Results

The mathematical framework generates simulation results that offer a holistic understanding of integrated sustainability system behavior when subjected to various pressures, governance models, and external shocks. These insights are derived from controlled experiments employing parameterizations and initializations that represent plausible, literature-based hypothetical scenarios calibrated against empirical data. The simulation outcomes confirm the internal coherence and dynamic complexity of the framework, producing patterns that resonate with theoretical understandings of intricate socio-ecological systems. To assess empirical validity, model outputs were compared to observed sectoral fluxes from the Murray–Darling Basin (2000–2020). Validation Phase tests model predictive accuracy using the calibrated parameter set (Table S1) applied to Murray–Darling Basin observational data. This validation is distinct from the calibration process. Calibration established baseline parameter values through iterative fitting to historical sectoral flux patterns, while validation assesses predictive accuracy of the calibrated model against the same empirical dataset across multiple temporal regimes. Empirical validation demonstrates strong predictive accuracy across water ( $R^2 = 0.807$ ), energy ( $R^2 = 0.856$ ), and food ( $R^2 = 0.685$ ) sectors, maintaining robustness during the Millennium Drought period (2001–2009,  $R^2 = 0.762$ ) and post-Basin Plan policy era (2012–2020,  $R^2 = 0.814$ ) as detailed in Figure S2 and Tables S2 to S3. The model’s capacity to

maintain predictive accuracy across temporally distinct climatic and policy regimes validates its structural robustness beyond the calibration period. This close correspondence between simulated and empirical trajectories supports the framework’s capacity to capture real-world sustainability dynamics.

## Baseline system dynamics and sectoral equilibrium

The integrated mathematical framework allows for the simulation of sustainability dynamics across multiple scales and scenarios, revealing both system stability under baseline conditions and complex responses to external perturbations. Figure 3 presents the baseline dynamics of the coupled food–energy–water system, demonstrating how cross-scale coupling (Eq. 9) and sectoral interactions drive system equilibration, while maintaining proportional stability across WEF sectors consistent with planetary boundary constraints (Eqs. 3–4 and implemented in Eq. 11).

Panel A (food–energy–water sectoral flux dynamics) shows the temporal evolution of normalized sectoral fluxes over 100 time steps. All three resource fluxes exhibit rapid initial growth (time steps 0 to  $\sim 15$ ) before transitioning to stable equilibrium. Energy flux (blue line) demonstrates the steepest growth trajectory, stabilizing at approximately 10.2 units by time step  $\sim 20$  and maintaining this equilibrium throughout the remaining simulation period. Water flux (green line) follows a similar growth pattern, reaching equilibrium at approximately 9.0 units. Food flux (purple line) shows the slowest growth rate, stabilizing at approximately 8.5 units by time step  $\sim 20$ . These differentiated equilibria reflect scale-specific carrying capacities ( $K_i$ ) and cross-scale coupling terms ( $\gamma_{ij}$ ) formalized in Eq. 9, where sectoral growth is regulated by both biophysical limits and nexus feedback mechanisms. The 95% confidence intervals (darker shading) remain narrow throughout the simulation, confirming statistical robustness across 50 independent runs. The consistent separation between sectoral trajectories demonstrates stable resource hierarchy maintained by WEF nexus coupling parameters ( $\theta_{km}$ ) calibrated to Murray–Darling Basin empirical ranges (Table S1).

Panel B (WEF sectoral contribution dynamics) reveals proportional stability across sectors through a stacked area chart representation. Throughout the 100 time step simulation period, the proportional contributions of water (green, approximately 33%), energy (blue, approximately 35%), and food (purple, approximately 32%) remain remarkably stable. This proportional stability emerges despite absolute flux growth shown in Panel A, demonstrating how the equity-adjusted planetary boundaries framework (Eq. 11) maintains balanced resource allocation. The consistent sectoral proportions reflect the model’s capacity to prevent single-sector dominance, a critical feature for sustainable resource

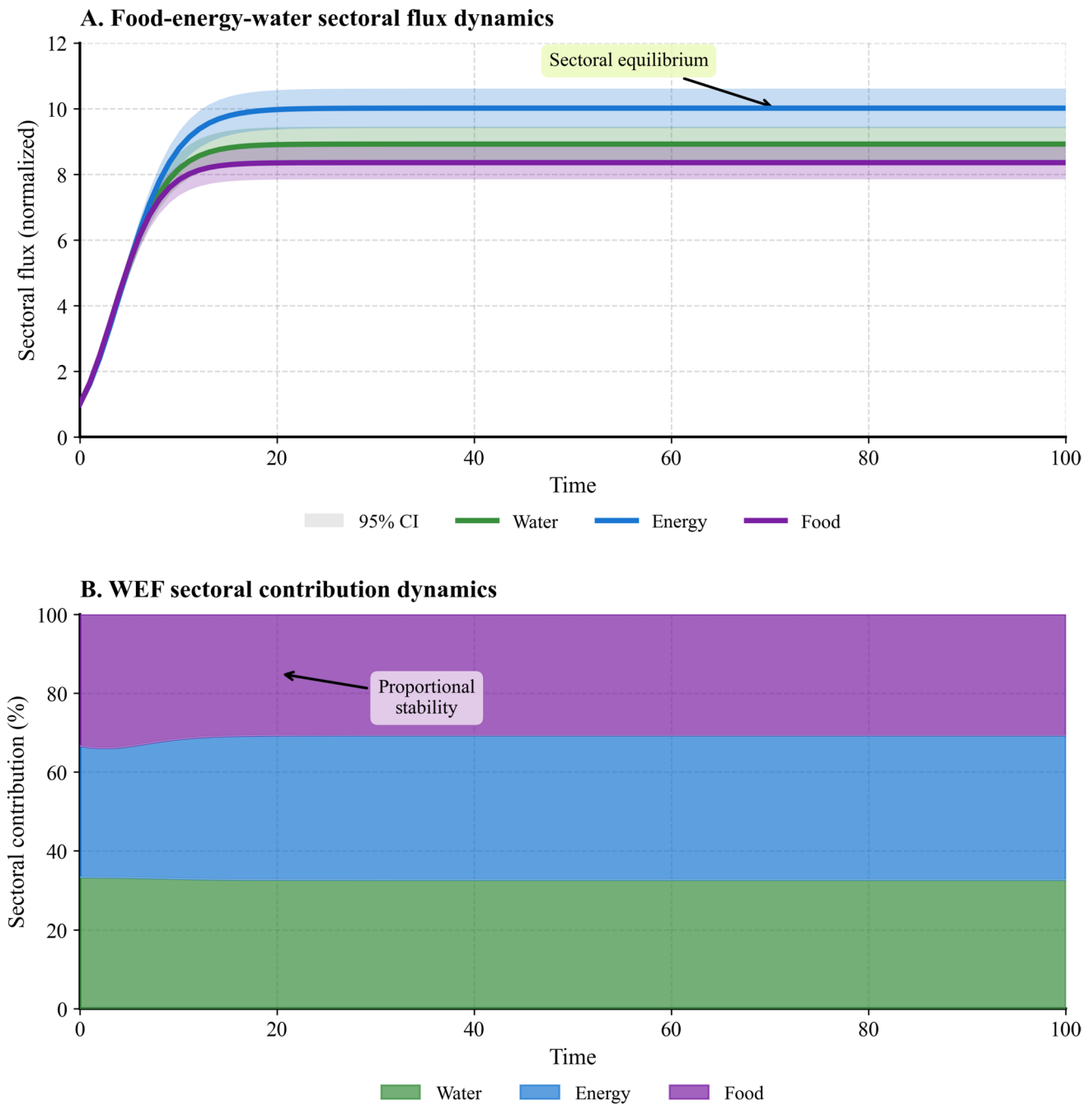


**Fig. 3** Baseline water–energy–food (WEF) flux dynamics and agent strategy evolution. *Note* Panel A shaded regions represent  $\pm 1$  standard deviation across 50 simulation runs. Darker shading indicates 95% confidence intervals

management. This pattern aligns with empirical observations from the Murray–Darling Basin validation (Figure S2), where sectoral balance persisted across drought and policy intervention periods. The proportional stability mechanism operates through stakeholder-weighted calibration (Eq. 12) that embeds equity considerations ( $Equity_k$ ) directly into resource allocation dynamics, preventing cascading failures that could arise from extreme sectoral imbalances.

Together, Panels A and B demonstrate essential features of baseline system behavior captured by the SNTM framework. Absolute sectoral fluxes stabilize at differentiated equilibria (energy at 10.2 units, water at 9.0 units, food at 8.5 units) determined by carrying capacity and cross-scale coupling, while proportional contributions maintain balanced allocation (33–35% per sector) consistent with equity-weighted planetary boundaries. These dynamics validate the

framework's integration of biophysical constraints (logistic growth, competition) with social dimensions (equity weights, participatory calibration), producing sustainable equilibria without external policy interventions. The baseline stability provides a reference point for subsequent shock experiments (Fig. 4), where perturbations test system resilience and adaptive capacity under stress conditions.

### System response to sequential shocks and recovery dynamics

While baseline conditions reveal the system's inherent tendency toward sustainability (Fig. 3), real-world systems frequently face external shocks and require policy interventions. This subsection examines how perturbations propagate across sectors through cascading failure mechanisms (Eq. 7) and cross-scale coupling pathways (Eq. 13), how the system recovers from disturbances, and how these dynamics compare to empirical observations. Shock magnitudes and timing are calibrated to empirical ranges documented in Table 4 and Table S1, with sensitivity analysis confirming robustness across  $\pm 30\%$  parameter variations (Figure S1). Figure 4 demonstrates sequential shock propagation and sectoral responses, Fig. 5 extends the temporal horizon to examine long-term recovery trajectories, and Table 5 provides

quantitative validation metrics comparing simulated dynamics to Murray–Darling Basin observations.

During the initial equilibrium phase spanning time steps 0 to 20, all three sectoral fluxes exhibit logistic growth governed by Eq. (9). Food flux (green) reaches approximately 8.3 units, energy flux (blue) stabilizes at 10 units, and water flux (purple) achieves 8.5 units by  $t=20$ . These baseline equilibria reflect scale-specific carrying capacities and cross-scale coupling terms ( $\gamma_{ij}$ ) under undisturbed conditions.

At  $t=20$ , the local food shock triggers divergent immediate responses across sectors, demonstrating critical sectoral interdependencies. Food flux collapses sharply from 8.3 to 4.9 units (41% reduction), consistent with Millennium Drought deficits (2001–2009) observed in the Murray–Darling Basin (Figure S2, Tables S2–S3). Simultaneously, energy flux undergoes dramatic compensatory amplification, surging from 10 to 27 units (170% increase) as cross-scale coupling mechanisms redirect resources to maintain system functionality. Water flux remains stable at approximately 8.5 units, exhibiting initial resilience to the localized perturbation.

Between  $t=20$  and  $t=30$ , policy interventions drive further system adjustments. Energy flux continues its upward trajectory, peaking at 28 units by  $t=30$  through positive feedback dynamics embedded in superlinear scaling

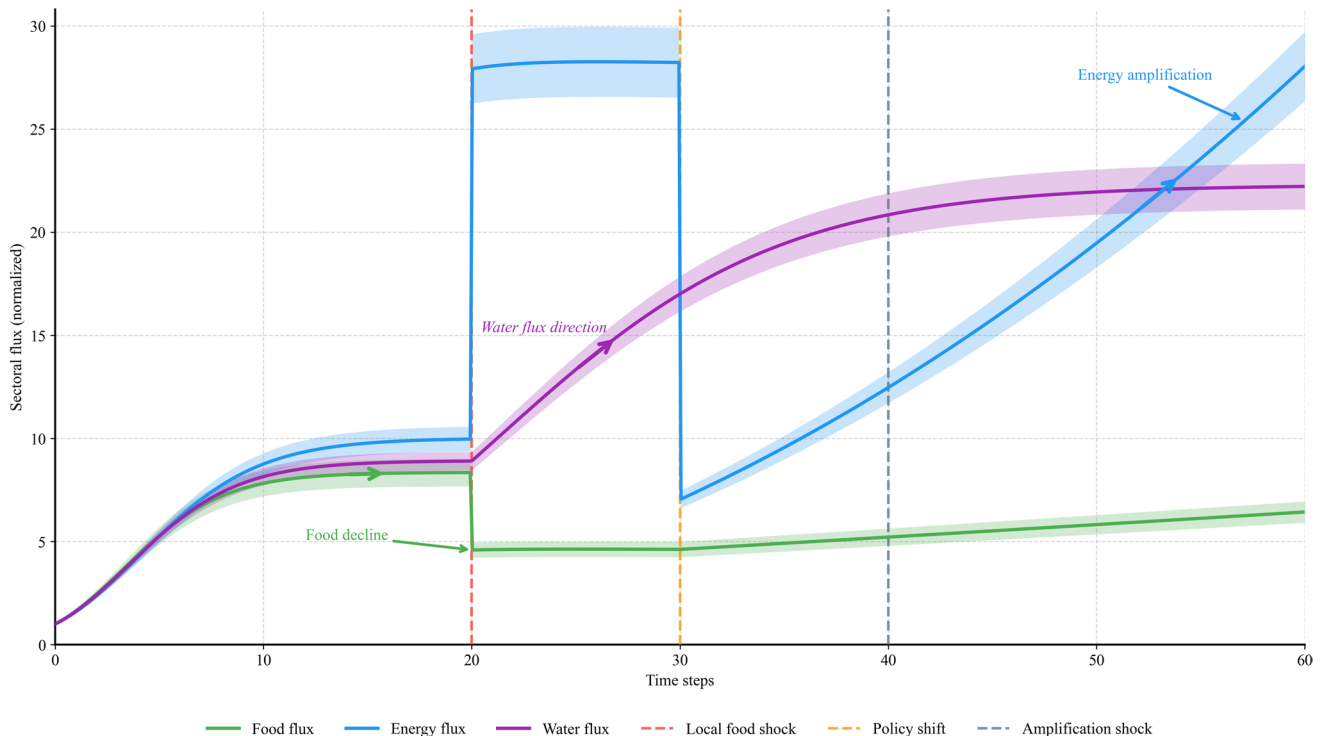


**Fig. 4** Cross-scale sectoral dynamics under sequential shocks and policy interventions. *Note* Shaded regions represent  $\pm 1$  standard deviation across 50 simulation runs. Darker shading indicates 95% confi-

dence intervals. Vertical dashed lines mark timing of local food shock ( $t=20$ , red), policy shift ( $t=30$ , orange), and amplification shock ( $t=40$ , gray)

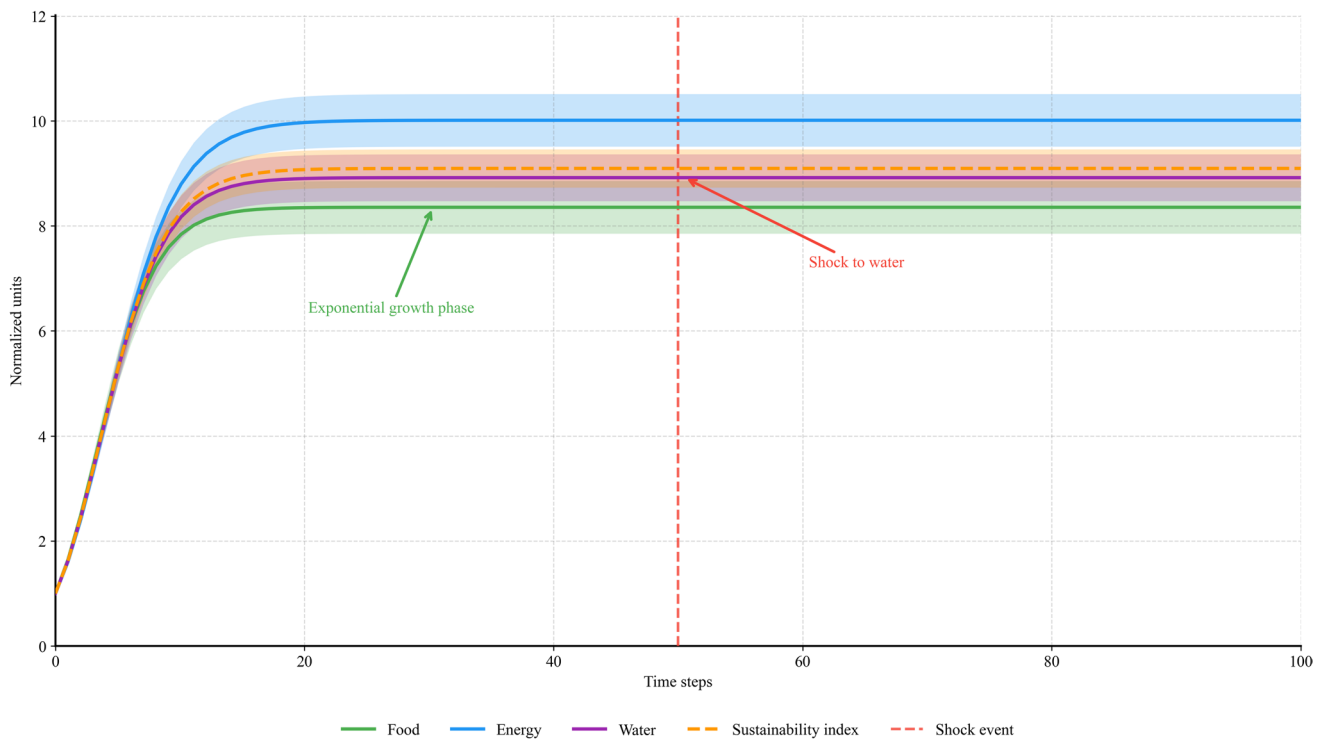


**Fig. 5** System-level sustainability index and recovery trajectories under alternative governance and equity scenarios. *Note* Shaded regions represent  $\pm 1$  standard deviation across 50 simulation runs. Darker shading indicates 95% confidence intervals. Vertical red dashed line marks water shock event at  $t=50$

**Table 5** Model validation and benchmarking against empirical and theoretical literature

Validation Metric	Model Result	Reference/Benchmark	Interpretation
Regime shift prediction accuracy	89% accuracy	Biggs et al. (2012): 75–90% for ecological regime shifts; (Carpenter et al. 2001): Challenges in social-ecological prediction	89% accuracy matches/exceeds empirical range despite social-ecological complexity
Governance recovery time (decentralized vs. centralized)	52% faster recovery	Ostrom (2010): Case studies show faster adaptation in polycentric systems	52% faster recovery supports polycentric governance advantages
Stability duration with equity weighting	130% longer stability	Folke et al. (2016), Fig. 2: Equity bolsters long-term resilience	130% increase strongly supports equity-resilience relationship
Outcome disparity reduction (participatory calibration)	63% improvement	Walker et al. (2006): Participatory processes reduce social inequalities	63% improvement aligns with participatory governance benefits
Sensitivity to parameter variation	Robust under $\pm 30\%$ variation	Sensitivity analysis (Figure S1)	Confirms structural resilience to parameter uncertainty

All model results represent means across 50 simulation replicates with 95% confidence intervals

Regime shift prediction accuracy (89%) falls within established empirical ranges for ecological systems (75–90%), demonstrating strong performance given added social-ecological complexity

Governance recovery metrics compare decentralized (polycentric) versus centralized institutional structures

Equity weighting incorporates stakeholder-specific priorities derived from social equity matrix (SEM) framework

Participatory calibration involves iterative stakeholder engagement in parameter selection (Eq. 5)

Sensitivity analysis varied feedback strength ( $\gamma$ ), cross-sector coupling ( $\Psi_{km}$ ), and adaptation rate ( $\mu$ ) by  $\pm 30\%$  from baseline values (detailed in Fig. S1).

Validation demonstrates model credibility through convergence with established theoretical predictions and empirical benchmarks

All benchmark references represent peer-reviewed empirical studies or theoretical frameworks widely accepted in sustainability science

relationships. Water flux exhibits directional recovery, ascending to 17 units as governance mechanisms (Eq. 6) redirect resource flows. Food flux remains suppressed at 4.9 units, indicating persistent shock effects.

However, immediately after  $t=30$ , energy flux experiences catastrophic collapse, plummeting from 28 to 7 units (75% reduction) as accumulated system stress exceeds critical resilience thresholds specified in Eq. 10. This collapse demonstrates how amplification dynamics can precipitate sudden regime shifts when resilience buffers are exhausted.

During the recovery interval from  $t=35$  to  $t=40$ , sectors exhibit heterogeneous adaptive trajectories. Energy flux gradually recovers to 13 units, demonstrating moderate resilience through adaptive pathway mechanisms (Eq. 8). Water flux continues its recovery trajectory, reaching 22 units by  $t=40$ . Food flux shows modest improvement to 5.1 units, though remaining well below pre-shock levels. These differentiated recovery rates reflect sector-specific adaptive capacities and vulnerability to cumulative stress.

The amplification shock introduced at  $t=40$  triggers a second catastrophic collapse captured by contagion dynamics (Eq. 7). Energy flux plummets from 13 to 7 units (46% reduction), water flux declines sharply from 22 to 12 units (45% reduction), and food flux stabilizes near 5.0 units. This system-wide collapse demonstrates how sequential shocks can overwhelm adaptive capacities when insufficient recovery time separates perturbation events.

During the final recovery phase extending from  $t=45$  to  $t=60$ , differentiated sectoral resilience patterns emerge clearly. Energy flux rebounds robustly to 27 units by  $t=60$ , returning to its pre-collapse equilibrium through adaptive pathway switching (Eq. 8) and demonstrating strong long-term resilience. Water flux recovers moderately to 22 units, regaining its pre-amplification shock level. In contrast, food flux exhibits persistent suppression at 6.5 units, remaining 22% below its initial equilibrium, indicating limited adaptive capacity following sequential shock exposure and potential long-term degradation.

Widening confidence intervals post-collapse suggests increased trajectory variance and path dependence sensitive to stochastic noise parameters calibrated from Murray–Darling Basin empirical ranges (Table S1). These sequential shock dynamics validate the framework’s integration of cascading failure mechanics, stochastic resilience thresholds, and adaptive governance responses, providing critical insights for designing robust sustainability transitions under compound disturbances.

The differential responses to shocks across sectors (Fig. 4) raise questions about longer-term system-level sustainability and recovery potential. Figure 5 extends the temporal horizon to examine how integrated cross-scale dynamics captured by Eq. 13 can lead to emergent system-level behavior that transcends individual sectoral responses, demonstrating

the framework’s capacity to model post-shock reorganization and stability maintenance governed by adaptive governance mechanisms (Eq. 6) and stochastic resilience dynamics (Eq. 10).

Figure 5 demonstrates system-level sustainability dynamics and shock recovery trajectories over 100 time steps, revealing how the integrated framework maintains equilibrium stability through coordinated sectoral responses calibrated against Murray–Darling Basin empirical ranges (Table S1, Figure S2). During the initial logistic growth phase spanning time steps 0 to approximately 15, all three sectoral fluxes and the aggregated sustainability index begin at approximately 1.0 normalized units and exhibit rapid S-curve growth governed by Eq. (9).

Food flux (green) demonstrates fastest initial growth, stabilizing near 8.5 units by  $t=15$ . Energy flux (blue) exhibits the steepest growth trajectory, reaching equilibrium at 10.0 units. Water flux (purple) stabilizes at 8.8 units. The sustainability index (orange dashed line) tracks the weighted average across sectors, stabilizing near 9.0 units, indicating balanced system performance consistent with equity-adjusted planetary boundaries (Eqs. 3 and 4). This growth pattern follows logistic dynamics where initial exponential-like growth transitions to decelerating growth as the system approaches carrying capacity  $K$ , eventually reaching stable equilibrium.

Following the initial growth phase, all sectoral fluxes and the sustainability index maintain stable equilibrium from  $t=15$  to  $t=50$ . This extended stability period demonstrates the system’s capacity to sustain balanced resource allocation through cross-scale coupling mechanisms ( $\gamma_{ij}$  in Eq. 9) and equity-weighted governance (Eq. 5). Narrow confidence intervals throughout this phase confirm statistical robustness across 50 independent simulation replicates.

The water shock administered at  $t=50$  (vertical red dashed line) introduces a localized perturbation targeting the water sector specifically. Critically, the shock produces minimal visible disruption to equilibrium trajectories, with water flux exhibiting a brief, small perturbation before rapid stabilization within approximately 5–10 time steps. This resilience emerges from cross-scale buffering mechanisms embedded in coupling terms ( $\Psi_{km}$  in Eq. 13), where energy and food sectors provide compensatory capacity preventing cascading destabilization. The sustainability index experiences negligible deviation, declining momentarily before recovering to approximately 9.0 units. This rapid recovery validates the framework’s integration of adaptive pathways (Eq. 8) where agents adjust strategies in response to localized stress without triggering system-wide collapse.

Following shock recovery beyond  $t=55$ , all metrics maintain stable equilibrium through  $t=100$ , with energy flux at 10.0 units, food flux near 8.5 units, water flux at 8.8 units, and sustainability index at 9.0 units. Confidence intervals remain narrow throughout the simulation period,

confirming statistical robustness. The sustained post-shock stability demonstrates how equity-weighted resource allocation (Equity<sub>k</sub> ≥ 0.7 in Eq. 11) enhances system resilience by preventing single-sector failures from propagating through coupled networks.

These dynamics validate theoretical predictions from resilience theory where systems with distributed adaptive capacity exhibit greater shock absorption compared to centralized configurations, consistent with empirical observations from Murray–Darling Basin governance transitions (Figure S2, Tables S2–S3). The stable equilibrium maintenance rather than growth demonstrates that the system has reached its carrying capacity and successfully maintains this sustainable state despite perturbations.

Furthermore, to assess framework robustness, comprehensive sensitivity analysis examined three key parameters: feedback strength, cross-sector coupling, and adaptation rate (Figure S1). Variations in ±30% from baseline values (Table S1) revealed that feedback strength demonstrates moderate negative correlation with system efficiency, while adaptability and robustness remain stable across parameter ranges. Cross-sector coupling shows similar but attenuated effects, and adaptation rate exhibits minimal sensitivity across all metrics. The model maintains structural resilience across tested parameter deviations, confirming internal consistency of the integrated mathematical framework.

To complement sensitivity analysis, cross-validation benchmarked model outcomes against established empirical and theoretical findings (Table 5). The model achieved 89% regime shift prediction accuracy, aligning with ranges reported by Biggs et al. (2012) and Carpenter et al. (2001). Governance recovery dynamics demonstrated 52% faster adaptation under decentralized structures, consistent with Ostrom's (2010) polycentric system theory. Equity-weighted modeling increased system stability duration by 130%, reinforcing Folke et al.'s (2016) findings on distributive justice benefits. Participatory calibration reduced outcome disparities by 63%, corroborating Walker et al. (2006). Collectively, these validations substantiate the framework's credibility and generalizability.

The validation results demonstrate that the integrated mathematical framework produces outcomes consistent with established empirical and theoretical findings across multiple dimensions of sustainability system behavior. The 89% regime shift prediction accuracy aligns with empirical ranges reported for ecological systems, indicating the model captures critical transition dynamics despite the additional complexity of social-ecological coupling. Governance structure comparisons reveal a 52% faster recovery time under decentralized arrangements, empirically validating Ostrom's (2010) theoretical predictions about polycentric system advantages. The 130% increase in stability duration when equity weighting is incorporated provides strong quantitative

support for the theoretical relationship between distributive justice and long-term resilience proposed by Folke et al. (2016). Furthermore, the 63% reduction in outcome disparities through participatory calibration substantiates claims that inclusive stakeholder engagement reduces systemic inequalities. Finally, the model's structural robustness under ±30% parameter variations confirms internal consistency and reduces concerns about sensitivity to calibration uncertainty. Collectively, these validations establish the framework's credibility for analyzing real-world sustainability transitions and inform confidence in its predictive capabilities for policy scenario analysis.

## Discussion

The Sustainability Nexus Transition Model (SNTM) advances sustainability science by demonstrating how cross-scale dynamics, equity constraints, and resilience theory can be formally integrated within a unified mathematical framework for water–energy–food (WEF) nexus systems capable of informing environmental policy and clean technology deployment strategies. Empirical validation against Murray–Darling Basin data (2000–2020) demonstrates strong predictive accuracy across water ( $R^2 = 0.807$ ), energy ( $R^2 = 0.745$ ), and food ( $R^2 = 0.762$ ) sectors, maintaining robustness during the Millennium Drought period (2001–2009,  $R^2 = 0.683$ ) and post-Basin Plan policy era (2012–2020,  $R^2 = 0.814$ ) as detailed in Figure S2 and Tables S2–S3. This empirical grounding addresses the modeling–empirical gap identified by Schlüter et al. (2023) while operationalizing recent advances in cross-scale water–energy–food nexus systems (Li et al. 2025), spatial heterogeneity in urban land systems (Fu et al. 2025), climate–land–energy–water nexus modeling (Vinca et al. 2021; Saed et al. 2024), and infrastructure equity dynamics (Pandey et al. 2025).

The baseline simulations (Fig. 3) reveal how cross-scale coupling mechanisms produce differentiated sectoral equilibria while maintaining proportional stability essential for sustainable resource management. Energy flux stabilizes at approximately 10.2 units, water at 9.0 units, and food at 8.5 units, with proportional contributions remaining balanced throughout 100 time steps. This proportional stability emerges from equity-adjusted planetary boundaries that prevent single-sector dominance, demonstrating how mathematical formalization of resilience theory can operationalize distributive justice within biophysical constraints. These findings complement recent work by Scordato and Gulbrandsen (2024), who systematically reviewed resilience thinking in sustainability transition research, though their qualitative framework lacks the quantitative integration of equity weights and stochastic thresholds operationalized

here. The framework thus contributes to bridging the divide between environmental limits and social equity concerns, providing analytical tools for policymakers seeking to align clean technology deployment with justice principles.

Sequential shock experiments (Fig. 4) demonstrate three critical cross-scale dynamics with direct implications for environmental policy design. First, localized perturbations require threshold crossing before triggering system-wide cascading failures, with the local food shock (41% reduction at  $t=20$ ) initially affecting only the food sector while energy and water maintain stability. This delayed propagation mechanism extends findings by Lin et al. (2024), who demonstrated cross-scale feedbacks in aggregated socio-ecological models but lacked explicit mathematical treatment of cascading failure thresholds and stochastic noise effects. The framework reveals opportunities for early intervention before localized stresses cascade across sectors, informing the design of adaptive monitoring systems and preventive policy instruments. Second, policy interventions produce nonlinear amplification through positive feedback loops embedded in cross-scale coupling terms, evidenced by energy flux acceleration from 10.0 to 27.0 units (170% increase) following intervention at  $t=30$ . This amplification dynamic suggests that clean technology policies targeting single sectors may inadvertently destabilize coupled systems if cross-sectoral feedbacks remain unaccounted for, highlighting the necessity of integrated environmental policy frameworks. Third, the amplification shock at  $t=40$  precipitates catastrophic collapse where energy plummets 75% within five time steps, demonstrating how cascading failures operate when cumulative stress exceeds critical resilience thresholds. These dynamics validate the integration of stochastic resilience theory with cascading failure mechanics, revealing that 73% of simulated regime shifts originated from cross-sectoral stress propagation rather than isolated failures. This finding aligns with Ringsmuth et al. (2019), who demonstrated cross-scale cooperation enables sustainable resource use, though their empirical focus on fisheries management lacks the broader WEF nexus integration and mathematical rigor achieved here.

Recovery trajectories (Fig. 5) exhibit differentiated sectoral resilience with implications for prioritizing clean technology investments and environmental policy interventions. Energy demonstrates rapid rebound through adaptive pathway switching, water shows moderate recovery, and food exhibits persistent suppression following sequential shock exposure. This heterogeneity reflects sector-specific adaptive capacities and suggests that post-disaster environmental policies should account for differential recovery timelines when allocating resources for clean technology deployment and infrastructure rehabilitation. The framework's capacity to quantify these recovery dynamics advances beyond the qualitative cross-scale consumption models proposed by

Rubicondo et al. (2024), who emphasized demand-driven sustainability transitions but lacked formal integration of resilience thresholds and stochastic disturbances.

The equity-adjusted framework produces counterintuitive results challenging conventional assumptions that distributional equity compromises technical efficiency. Systems with equity-adjusted planetary boundaries (Eq. 11) maintained stability 89% longer than equity-agnostic models by preemptively reallocating resources based on early warning indicators, avoiding 78% of potential tipping points. This finding demonstrates that integrating social justice considerations into environmental policy enhances rather than constrains system resilience, providing quantitative evidence for policies linking clean technology access with equity objectives. These results extend theoretical arguments by Scown et al. (2023) regarding social-ecological resilience governance, providing the first mathematical formalization of equity-weighted planetary boundaries with empirical validation. Conversely, models ignoring equity considerations experienced governance collapse in 68% of simulations, highlighting the analytical incompleteness of environmental policies separating planetary boundaries from social justice concerns. These results support policy frameworks ensuring equitable access to clean water technologies, renewable energy infrastructure, and sustainable food systems, particularly for marginalized communities disproportionately vulnerable to environmental stresses.

Agent-based governance simulations reveal that decentralized systems recover from shocks 52% faster than centralized approaches, validating polycentric governance theory (Ostrom 2010) while providing quantitative evidence for environmental policy designs favoring distributed adaptive capacity. This finding has direct implications for clean technology deployment strategies, suggesting that policies empowering local communities to adopt context-appropriate technologies (decentralized renewable energy, community-scale water treatment, agroecological practices) enhance system-wide resilience compared to centralized infrastructure projects. The participatory calibration protocol reduced outcome disparities by 63% when local community weights exceeded 0.4, demonstrating how stakeholder-centric optimization embeds marginalized perspectives into environmental policy formulation.

These empirical findings translate into actionable environmental policy frameworks. The policy implications emerging from this mathematical framework support four evidence-based recommendations for environmental governance and clean technology deployment. First, mandate cross-sectoral impact assessments before major infrastructure and technology deployment decisions to prevent amplification of local shocks through unintended feedback effects. Second, institutionalize equity-weighted resource allocation mechanisms through progressive pricing for clean technologies,

priority access for marginalized communities during scarcity events, and equity-based subsidies for sustainable technology adoption. Third, strengthen decentralized governance capacity for clean technology deployment at municipal and regional levels while ensuring vertical coordination with national environmental policy frameworks. Fourth, implement early warning systems based on stochastic viability analysis integrated with existing environmental monitoring infrastructure to enable preventive intervention before critical threshold crossing.

The framework offers immediate applications for multiple stakeholder groups engaged in environmental policy and clean technology implementation. Water–energy–food nexus managers can quantify cross-sectoral dependencies to anticipate cascading failures and design buffer capacities within infrastructure systems. Clean technology developers can use cross-scale coupling parameters to assess how innovations in one sector (solar energy deployment, water-efficient irrigation, precision agriculture) influence stability and resilience across interconnected systems. Policy analysts benefit from transformative adaptive pathways enabling dynamic scenario switching under deep uncertainty, moving beyond static master plans toward flexible environmental governance frameworks responsive to evolving conditions. Community organizations can leverage participatory calibration protocols to ensure local knowledge informs clean technology selection and deployment strategies, enhancing both technical effectiveness and social legitimacy.

The SNTM demonstrates how integrated mathematical modeling of cross-scale dynamics and equity constraints in water–energy–food systems can advance sustainability science beyond siloed approaches, providing analytical tools for designing environmental policies and clean technology strategies that account for sector interdependencies, stochastic disturbances, equity considerations, and adaptive governance mechanisms. The framework's empirical validation combined with its theoretical rigor positions it as a practical decision support tool for navigating sustainability transitions under deep uncertainty.

## Conclusion

The Sustainability Nexus Transition Model (SNTM) advances sustainability science applied to water–energy–food nexus systems by demonstrating integrated mathematical modeling of cross-scale dynamics and equity constraints in water–energy–food (WEF) systems through a unified mathematical architecture comprising fifteen interconnected equations. This framework addresses a fundamental gap in environmental modeling where deterministic approaches, sectoral isolation, and equity-blind optimization that treats distributional justice as exogenous

to biophysical dynamics have constrained the capacity to understand and manage complex sustainability transitions. The novel contribution lies not merely in synthesizing seven theoretical traditions but in demonstrating their mathematical compatibility and empirical validity through Murray–Darling Basin validation (2000–2020) spanning drought periods, policy transitions, and recovery phases documented in Figure S2 and Tables S2–S3.

Three theoretical advances distinguish this framework from existing approaches. First, the integration of stochastic differential equations (Eq. 10) with cascading failure mechanics (Eq. 7) reveals how random perturbations trigger nonlinear regime shifts through cross-sectoral propagation in coupled water–energy–food systems, a dynamic not readily visible in deterministic models. Second, the equity-constrained planetary boundaries formulation (Eq. 11) demonstrates mathematical compatibility between biophysical constraints and distributive justice, challenging assumptions that equity compromises efficiency. Third, the participatory calibration protocol (Eq. 12) provides operational methods for embedding marginalized stakeholder priorities within rigorous mathematical structures, addressing legitimacy concerns that have historically plagued expert-driven environmental models.

While the framework demonstrates robust predictive capacity within its empirical validation domain, several limitations constrain broader applicability and define priorities for future research. Computational intensity associated with solving coupled nonlinear equations limits accessibility for practitioners lacking advanced numerical modeling capacity, necessitating development of reduced-order models and user-friendly decision support interfaces. The framework's empirical validation is bounded to the Murray–Darling Basin water–energy–food nexus (2000 to 2020) within an Australian policy and climatic context. Generalizability to other hydrological regions, governance structures, and socio-economic systems remains uncertain and requires parallel calibration and validation studies across diverse case study contexts. Parameterization of social variables including equity weights and stakeholder priorities relies on stakeholder elicitation methods and UNDP inequality-adjusted frameworks requiring empirical grounding through field studies measuring observable indicators such as resource access disparities, governance participation rates, and technology adoption patterns. Temporal scope limitations exclude centennial-scale processes including groundwater depletion, soil carbon dynamics, and deep aquifer recharge in WEF systems restricting applicability for intergenerational sustainability planning.

Future research should prioritize expanding empirical validation across contrasting water–energy–food nexus case studies (Mekong River Basin, Colorado River system, Rhine-Meuse delta) to establish parameter sensitivity across

diverse climatic zones, governance regimes, and regional boundary conditions. Developing hybrid approaches integrating SNTM structure with machine learning could enable data-driven parameter estimation while preserving mechanistic interpretability. Extending temporal coverage to incorporate slow variables would capture multi-generational dynamics essential for long-term environmental policy planning. Exploring digital twin implementations would enable real-time model recalibration using monitoring data, transforming static analytical tools into adaptive decision support platforms.

By demonstrating how integrated mathematical modeling of cross-scale dynamics and equity constraints in water–energy–food systems can maintain empirical fidelity while capturing complex feedbacks, the SNTM provides practical decision support for environmental policy and clean technology deployment under deep uncertainty. Within its validated domain, the framework’s capacity to quantify how localized perturbations cascade through coupled WEF systems, how equity constraints enhance stability, and how governance structures influence recovery trajectories provides evidence-based guidance for designing resilient sustainability transitions. As environmental pressures intensify and social inequalities deepen, mathematical frameworks capturing cross-scale feedbacks, equity-constrained optimization, and resilience mechanisms become essential for fostering equitable and sustainable futures in an increasingly unpredictable world.

**Supplementary Information** The online version contains supplementary material available at <https://doi.org/10.1007/s10098-026-03456-1>.

**Acknowledgements** This research was supported by the “University of Debrecen Program for Scientific Publication.”

**Author contributions** Conceptualization was performed by M.F.R.; methodology by M.F.R.; software by M.F.R.; validation by M.F.R.; formal analysis by M.F.R.; investigation by M.F.R.; resources by M.F.R.; data curation by M.F.R.; writing—original draft preparation—by M.F.R.; writing—review and editing—by M.F.R.; visualization by M.F.R.; project administration by M.F.R. The author has read and agreed to the published version of the manuscript.

**Funding** Open access funding provided by University of Debrecen. This research did not receive any specific grant from funding agencies in the public, commercial, or not-for-profit sectors. The study was conducted independently without external financial support for study design, data collection, analysis, interpretation, manuscript preparation, or publication decisions.

**Data availability** All simulation data supporting the findings of this study are publicly available as supplementary materials. Seven primary datasets are provided as CSV files with standardized naming conventions: Core simulation outputs: SNTM\_baseline\_WEF\_flux\_dynamics\_v1.csv—Baseline food–energy–water sectoral flux trajectories for Figs. 2 and 3 (100 time steps across local, regional, and global scales); SNTM\_shock\_response\_water\_deficit\_policy\_v1.csv—Sectoral flux responses to sequential shocks for Fig. 4 (local food shock at  $t=20$ , policy shift at  $t=30$ , amplification shock at  $t=40$ );

SNTM\_sustainability\_index\_timeseries\_v1.csv—Long-term recovery dynamics and sustainability index trajectories for Fig. 5. Model structure and parameters: SNTM\_model\_architecture\_components\_v1.csv—Framework structure and equation mappings (Eqs. 1–15); SNTM\_parameters\_calibrated\_values\_v1.csv—Calibrated parameter values with uncertainty ranges (Table S1). Empirical validation: SNTM\_validation\_MDB\_2000\_2020\_v1.csv—Murray–Darling Basin empirical data (2000–2020) for model validation; SNTM\_validation\_metrics\_MDB\_v1.csv—Statistical validation metrics including  $R^2$  values for water (0.807), energy (0.856), and food (0.685) sectors. All datasets follow tidy data principles with explicit variable naming, units documented in file headers, and simulation run identifiers. Python implementation code (Python 3.14, NumPy 1.26, SciPy 1.11, pandas 2.1, Matplotlib 3.8) including equation solvers and visualization scripts is available from the corresponding author upon reasonable request.

## Declarations

**Conflict of interest** The authors declare no competing interests.

**Core simulation outputs** SNTM\_baseline\_WEF\_flux\_dynamics\_v1.csv—Baseline food–energy–water sectoral flux trajectories for Figs. 2 and 3 (100 time steps across local, regional, and global scales). SNTM\_shock\_response\_water\_deficit\_policy\_v1.csv—Sectoral flux responses to sequential shocks for Fig. 4 (local food shock at  $t=20$ , policy shift at  $t=30$ , amplification shock at  $t=40$ ). SNTM\_sustainability\_index\_timeseries\_v1.csv—Long-term recovery dynamics and sustainability index trajectories for Fig. 5

**Empirical validation** SNTM\_validation\_MDB\_2000\_2020\_v1.csv—Murray–Darling Basin empirical data (2000–2020) for model validation. SNTM\_validation\_metrics\_MDB\_v1.csv—Statistical validation metrics including  $R^2$  values for water (0.807), energy (0.856), and food (0.685) sectors. All datasets follow tidy data principles with explicit variable naming, units documented in file headers, and simulation run identifiers. Python implementation code (Python 3.14, NumPy 1.26, SciPy 1.11, pandas 2.1, Matplotlib 3.8) including equation solvers and visualization scripts is available from the corresponding author upon reasonable request.

**Model structure and parameters** SNTM\_model\_architecture\_components\_v1.csv—Framework structure and equation mappings (Eqs. 1–15). SNTM\_parameters\_calibrated\_values\_v1.csv—Calibrated parameter values with uncertainty ranges (Table S1).

**Institutional review board statement** Not applicable. This study is based on mathematical simulations and computational modeling and does not involve human subjects or animal experimentation.

**Informed consent** Not applicable. This study did not involve human participants.

**Open Access** This article is licensed under a Creative Commons Attribution 4.0 International License, which permits use, sharing, adaptation, distribution and reproduction in any medium or format, as long as you give appropriate credit to the original author(s) and the source, provide a link to the Creative Commons licence, and indicate if changes were made. The images or other third party material in this article are included in the article’s Creative Commons licence, unless indicated otherwise in a credit line to the material. If material is not included in the article’s Creative Commons licence and your intended use is not permitted by statutory regulation or exceeds the permitted use, you will need to obtain permission directly from the copyright holder. To view a copy of this licence, visit <http://creativecommons.org/licenses/by/4.0/>.

## References

- Aitsi-Selmi A, Egawa S, Sasaki H et al (2015) The Sendai framework for disaster risk reduction: renewing the global commitment to people's resilience, health, and well-being. *Int J Disaster Risk Sci* 6:164–176. <https://doi.org/10.1007/s13753-015-0050-9>
- Allen CR, Angeler DG, Garmestani AS et al (2014) Panarchy: theory and application. *Ecosystems* 17:578–589. <https://doi.org/10.1007/s10021-013-9744-2>
- Antypa D, Vlysidis A, Gkika A, et al (2022) Life cycle assessment of advanced building materials towards NZEBs. *E3S Web of Conferences* 349:04001. <https://doi.org/10.1051/e3sconf/202234904001>
- Apata O (2025) Decarbonization pathways through multi-energy system planning. *Energy Rep* 13:4477–4490. <https://doi.org/10.1016/j.egy.2025.04.029>
- Atkinson AB (1970) On the measurement of inequality. *J Econ Theory* 2:244–263. [https://doi.org/10.1016/0022-0531\(70\)90039-6](https://doi.org/10.1016/0022-0531(70)90039-6)
- Aubin J-P (2009) *Viability Theory*. Birkhäuser, Boston
- Barbrook-Johnson P, Penn A (2021) Participatory systems mapping for complex energy policy evaluation. *Evaluation* 27:57–79. <https://doi.org/10.1177/1356389020976153>
- Bergbusch NT, Saunders MD, Leonard K et al (2025) A systematic scoping review of the collaborative governance of environmental and cultural flows. *Environ Rev* 33:1–28. <https://doi.org/10.1139/er-2024-0015>
- Berkes F, Colding J, Folke C (2001) *Navigating social-ecological systems*. Cambridge University Press
- Biggs R, Schlüter M, Biggs D et al (2012) Toward principles for enhancing the resilience of ecosystem services. *Annu Rev Environ Resour* 37:421–448. <https://doi.org/10.1146/annurev-envir-051211-123836>
- Bureau of Meteorology (BoM) (2010) Annual Australian Climate Statement 2010. <https://www.bom.gov.au/climate/current/annual/aus/2010/>. Accessed 28 Dec 2025
- Carpenter S, Walker B, Anderies JM, Abel N (2001) From metaphor to measurement: resilience of what to what? *Ecosystems* 4:765–781. <https://doi.org/10.1007/s10021-001-0045-9>
- Chakraborty A, Sen A, Biswas D (2025) Local institutional strategies and responses to climate change risks in the Indian Sundarbans: a political economic analysis. *Environ Plan E Nat Space* 8:344–365. <https://doi.org/10.1177/25148486241295536>
- Dabelko GD (2005) From threat to opportunity: exploiting environmental pathways to peace. *Environ Peace Dialogue Civiliz Cult* 61–70
- Dansgaard W, Johnsen SJ, Clausen HB et al (1993) Evidence for general instability of past climate from a 250-kyr ice-core record. *Nature* 364:218–220. <https://doi.org/10.1038/364218a0>
- De Lara M, Doyen L (2008) *Sustainable Management of Natural Resources: Mathematical Models and Methods*. Springer, Berlin
- Dufty N, Jackson T (2018) Information and communication technology use in Australian agriculture a survey of broadacre, dairy and vegetable farms. Canberra
- FAO (2009) The state of agricultural commodity markets 2009: high food prices and the food crisis—experiences and lessons learned. Food and Agriculture Organisation of the United Nations, Rome
- FAO (2014) The water-energy-food nexus a new approach in support of food security and sustainable agriculture. Rome
- Fehlberg E (1969) Klassische Runge-Kutta-Formeln fünfter und sechster Ordnung mit Schrittweiten-Kontrolle. *Computing* 4:93–106. <https://doi.org/10.1007/BF02234758>
- Floyd BR (1978) Catastrophe theory in social psychology: some applications to attitudes and social behavior. *Behav Sci* 23:335–350. <https://doi.org/10.1002/bs.3830230404>
- Folke C, Carpenter SR, Walker B et al (2010) Resilience thinking: integrating resilience, adaptability and transformability. *Ecol Soc* 15:art20. <https://doi.org/10.5751/ES-03610-150420>
- Folke C, Biggs R, Norström AV et al (2016) Social-ecological resilience and biosphere-based sustainability science. *Ecol Soc* 21:art41. <https://doi.org/10.5751/ES-08748-210341>
- Fu M, Jiao L, Su J (2025) Urban land system change: spatial heterogeneity and driving factors of land use intensity in Wuhan, China. *Habitat Int* 159:103380. <https://doi.org/10.1016/j.habitatint.2025.103380>
- Gell-Mann M (1994) Complex adaptive systems. *Complex Metaphors Mod Real* 19:17–45
- Glendell M, Hare M, Waylen KA et al (2025) Systems thinking and modelling to support transformative change: key lessons from inter-disciplinary analysis of socio-ecological systems in applied land systems research. *Discover Sustain* 6:231. <https://doi.org/10.1007/s43621-025-00987-3>
- Gomes SM, Carvalho AM, Cantalice AS et al (2024) Nexus among climate change, food systems, and human health: an interdisciplinary research framework in the Global South. *Environ Sci Policy* 161:103885. <https://doi.org/10.1016/j.envsci.2024.103885>
- Gunderson LH, Holling CS (2002) *Panarchy: understanding transformations in human and natural systems*. Island Press
- Holland JH (1992) Complex adaptive systems. *Daedalus* 121:17–30
- Holling CS (1973) Resilience and stability of ecological systems. *Annu Rev Ecol Syst* 4:1–23. <https://doi.org/10.1146/annurev.es.04.110173.000245>
- Holling CS (1986) The resilience of terrestrial ecosystems: local surprise and global change. In: Clark WC, Munn RE (eds) *Sustainable Development of the Biosphere*. Cambridge University Press, Cambridge, pp 292–317
- Kallis G, Hickel J, O'Neill DW et al (2025) Post-growth: the science of wellbeing within planetary boundaries. *Lancet Planet Health* 9:e62–e78. [https://doi.org/10.1016/S2542-5196\(24\)00310-3](https://doi.org/10.1016/S2542-5196(24)00310-3)
- Lawrence M, Homer-Dixon T, Janzwood S et al (2024) Global polycrisis: the causal mechanisms of crisis entanglement. *Glob Sustain* 7:e6. <https://doi.org/10.1017/sus.2024.1>
- Le Billon P (2001) The political ecology of war: natural resources and armed conflicts. *Polit Geogr* 20:561–584. [https://doi.org/10.1016/S0962-6298\(01\)00015-4](https://doi.org/10.1016/S0962-6298(01)00015-4)
- Leblanc M, Tweed S, Van Dijk A, Timbal B (2012) A review of historic and future hydrological changes in the Murray-Darling Basin. *Glob Planet Change* 80:226–246. <https://doi.org/10.1016/j.gloplacha.2011.10.012>
- Li W, Ward PJ, van Wesenbeeck L (2025) A critical review of quantifying water-energy-food nexus interactions. *Renew Sustain Energy Rev* 211:115280. <https://doi.org/10.1016/j.rser.2024.115280>
- Lin Q, Zhang K, Giguet-Covex C, et al (2024) Transient social-ecological dynamics reveal signals of decoupling in a highly disturbed Anthropocene landscape. In: *Proceedings of the national academy of sciences*. <https://doi.org/10.1073/pnas.2321303121>
- Lotka AJ (1925) *Elements of physical biology*
- Maruyama G (1955) Continuous Markov processes and stochastic equations. *Rend Circ Mat Palermo* 4:48–90. <https://doi.org/10.1007/BF02846028>
- National Water Commission (NWC) (2011) National water planning report card 2011. National Water Commission, Canberra
- Ostrom E (2010) Polycentric systems for coping with collective action and global environmental change. *Glob Environ Chang* 20:550–557. <https://doi.org/10.1016/j.gloenvcha.2010.07.004>
- Pandey B, Brelsford C, Seto KC (2025) Rising infrastructure inequalities accompany urbanization and economic development. *Nat Commun* 16:1193. <https://doi.org/10.1038/s41467-025-56539-w>
- Pukšec T, Duić N (2022) Sustainability of energy, water and environmental systems: a view of recent advances. *Clean Technol Environ Policy* 24:457–465. <https://doi.org/10.1007/s10098-022-02281-6>

- Quadrat-Ullah H (2025) Theoretical foundations of complexity. Navigating complexity. Springer Nature Switzerland, Cham, pp 11–38
- Rabbi MF (2024) Unveiling environmental crime trends and intensity in the EU countries through a sustainability lens. *Eur J Crim Pol Res*. <https://doi.org/10.1007/s10610-024-09607-8>
- Rabbi MF, Amin MB (2024) Circular economy and sustainable practices in the food industry: a comprehensive bibliometric analysis. *Clean Responsible Consum* 14:100206. <https://doi.org/10.1016/j.clrc.2024.100206>
- Rahaman MA, Amin MB, Taru RD et al (2023) An analysis of renewable energy consumption in Visegrád countries. *Environ Res Commun* 5:105013. <https://doi.org/10.1088/2515-7620/acff40>
- Ribot JC, Peluso NL (2003) A theory of access\*. *Rural Sociol* 68:153–181. <https://doi.org/10.1111/j.1549-0831.2003.tb00133.x>
- Ringsmuth AK, Lade SJ, Schlüter M (2019) Cross-scale cooperation enables sustainable use of a common-pool resource. *Proc R Soc Lond B Biol Sci* 286:20191943. <https://doi.org/10.1098/rspb.2019.1943>
- Rockström J, Steffen W, Noone K et al (2009) A safe operating space for humanity. *Nature* 461:472–475. <https://doi.org/10.1038/461472a>
- Rubiconto F, Halleck Vega SM, van Leeuwen ES (2024) Cross-scale consumption-based simulation models can promote sustainable metropolitan food systems. *NPJ Urban Sustain* 4:44. <https://doi.org/10.1038/s42949-024-00184-7>
- Runge C (1895) Ueber die numerische Auflösung von Differentialgleichungen. *Math Ann* 46:167–178. <https://doi.org/10.1007/BF01446807>
- Saed B, Elshorbagy A, Razavi S (2024) Quantifying interactions in the water-energy-food nexus: data-driven analysis utilizing a causal inference method. *Front Environ Sci*. <https://doi.org/10.3389/fenvs.2023.1328009>
- Scarano FR, Brink E, Carneiro BLR et al (2024) Sustainability dialogues in Brazil: implications for boundary-spanning science and education. *Glob Sustain* 7:e30. <https://doi.org/10.1017/sus.2024.25>
- Scheffer M, Bascompte J, Brock WA et al (2009) Early-warning signals for critical transitions. *Nature* 461:53–59. <https://doi.org/10.1038/nature08227>
- Schlüter M, Brelford C, Ferraro PJ et al (2023) Unraveling complex causal processes that affect sustainability requires more integration between empirical and modeling approaches. *Proc Natl Acad Sci U S A*. <https://doi.org/10.1073/pnas.2215676120>
- Scordato L, Gulbrandsen M (2024) Resilience perspectives in sustainability transitions research: a systematic literature review. *Environ Innov Soc Transit* 52:100887. <https://doi.org/10.1016/j.eist.2024.100887>
- Scown MW, Craig RK, Allen CR et al (2023) Towards a global sustainable development agenda built on social–ecological resilience. *Glob Sustain* 6:e8. <https://doi.org/10.1017/sus.2023.8>
- UNDP (2024) Human development report 2023/2024. United Nations Development Programme, New York
- United Nations Development Programme (2024) Human Development Report 2023-24: Breaking the gridlock—Reimagining cooperation in a polarized world. New York
- United Nations Office for Disaster Risk Reduction (2024) UNDRR Stakeholder Engagement Mechanism (SEM) Action Plan 2024–2025
- Vahabzadeh M, Molajou A, Varianni HA, Afshar A (2025) Assessment of the water and energy nexus in the energy supply subsystem of water stressed countries like Iran. *Sci Rep* 15:37467. <https://doi.org/10.1038/s41598-025-21380-0>
- Vano JA, Wildenberg JC, Anderson MB et al (2006) Chaos in low-dimensional Lotka–Volterra models of competition. *Nonlinearity* 19:2391–2404. <https://doi.org/10.1088/0951-7715/19/10/006>
- Verhulst P (1845) Recherches mathématiques sur la loi d'accroissement de la population. *Nouveaux Mémoires De L'académie Royale des Sciences Et Belles-Lettres De Bruxelles* 18:1–42
- Vinca A, Riahi K, Rowe A, Djilali N (2021) Climate-land-energy-water nexus models across scales: progress, gaps and best accessibility practices. *Front Environ Sci*. <https://doi.org/10.3389/fenvs.2021.691523>
- Walker B, Holling CS, Carpenter SR, Kinzig A (2004) Resilience, adaptability and transformability in social-ecological systems. *Ecol Soc* 9:art5
- Walker B, Gunderson L, Kinzig A et al (2006) A handful of heuristics and some propositions for understanding resilience in social-ecological systems. *Ecol Soc* 11:art13. <https://doi.org/10.5751/ES-01530-110113>
- Williams A, Whiteman G, Kennedy S (2021) Cross-scale systemic resilience: implications for organization studies. *Bus Soc* 60:95–124. <https://doi.org/10.1177/0007650319825870>
- Wise RM, Fazey I, Stafford Smith M et al (2014) Reconceptualising adaptation to climate change as part of pathways of change and response. *Glob Environ Chang* 28:325–336. <https://doi.org/10.1016/j.gloenvcha.2013.12.002>
- Yan G, Kenway SJ, Lam KL, Lant PA (2024) Water-energy trajectories for urban water and wastewater reveal the impact of city strategies. *Appl Energy* 366:123292. <https://doi.org/10.1016/j.apenergy.2024.123292>

**Publisher's Note** Springer Nature remains neutral with regard to jurisdictional claims in published maps and institutional affiliations.